THE JOURNAL OF BIOLOGICAL CHEMISTRY VOL. 287, NO. 6, pp. 3642–3658, February 3, 2012

Second Extracellular Loop of Human Glucagon-like Peptide-1 Receptor (GLP-1R) Has a Critical Role in GLP-1 Peptide Binding and Receptor Activation*[S]

Received for publication, September 30, 2011, and in revised form, November 29, 2011 Published, JBC Papers in Press, December 6, 2011, DOI 10.1074/jbc.M111.309328

Cassandra Koole[‡], Denise Wootten[‡], John Simms[‡], Laurence J. Miller[§], Arthur Christopoulos[‡1], and Patrick M. Sexton[‡2]

From the [‡]Drug Discovery Biology, Monash Institute of Pharmaceutical Sciences and Department of Pharmacology, Monash University, Parkville, Victoria 3052, Australia and the [§]Department of Molecular Pharmacology and Experimental Therapeutics, Mayo Clinic, Scottsdale, Arizona 85259

Background: The ECL2 of family B GPCRs has been suggested to contribute to biological activity.
Results: Mutation of most ECL2 residues to alanine results in changes in binding and/or efficacy of GLP-1 peptide agonists.
Conclusion: The ECL2 of the GLP-1R is critical for GLP-1 peptide-mediated receptor activation and selective signaling.
Significance: This work reveals broad significance for ECL2 in maintaining receptor conformations driving selective signaling.

The glucagon-like peptide-1 receptor (GLP-1R) is a therapeutically important family B G protein-coupled receptor (GPCR) that is pleiotropically coupled to multiple signaling effectors and, with actions including regulation of insulin biosynthesis and secretion, is one of the key targets in the management of type II diabetes mellitus. However, there is limited understanding of the role of the receptor core in orthosteric ligand binding and biological activity. To assess involvement of the extracellular loop (ECL) 2 in ligand-receptor interactions and receptor activation, we performed alanine scanning mutagenesis of loop residues and assessed the impact on receptor expression and GLP-1(1–36)-NH_2 or GLP-1(7–36)-NH_2 binding and activation of three physiologically relevant signaling pathways as follows: cAMP formation, intracellular Ca^{2+} (Ca^{2+}_i) mobilization, and phosphorylation of extracellular signal-regulated kinases 1 and 2 (pERK1/2). Although antagonist peptide binding was unaltered, almost all mutations affected GLP-1 peptide agonist binding and/or coupling efficacy, indicating an important role in receptor activation. However, mutation of several residues displayed distinct pathway responses with respect to wild type receptor, including Arg-299 and Tyr-305, where mutation significantly enhanced both GLP-1(1–36)-NH_2- and GLP-1(7–36)-NH_2-mediated signaling bias for pERK1/2. In addition, mutation of Cys-296, Trp-297, Asn-300, Asn-302, and Leu-307 significantly increased GLP-1(7–36)-NH_2-mediated signaling bias toward pERK1/2. Of all mutants studied, only mutation of Trp-306 to alanine abolished all biological activity. These data suggest a critical role of ECL2 of the GLP-1R in the activation transition(s) of the receptor and the importance of this region in the determination of both GLP-1 peptide- and pathway-specific effects.

GPCRs[3] are the largest family of transmembrane (TM)-spanning proteins, accounting for ~1% of the human genome, and are the leading target of marketed therapeutics (1, 2). Family B peptide hormone receptors are a small subfamily of GPCRs that include receptors for secretin, calcitonin, vasoactive intestinal polypeptide, pituitary adenylate cyclase-activating polypeptide, corticotrophin-releasing factor, parathyroid hormone, gastric inhibitory polypeptide, glucagon, and glucagon-like peptides (GLPs). Each receptor possesses a characteristically large and sequence-divergent extracellular N-terminal domain; however, there is conservation of key residues, including three disulfide bonds within this domain, that aids in stability and confers similarities in secondary structure (3, 4). The widely accepted peptide-receptor binding model for family B GPCRs is the two domain model, whereby the α-helical C terminus of the endogenous ligand interacts with the N-terminal domain of the receptor, and the N terminus of the peptide interacts with the core domain of the receptor, which includes both the extracellular loops and TM bundle (5–7). Generically, the N-terminal domain of the receptor is primarily responsible for ligand recognition and specificity, whereas the core of the receptor has a major influence in signaling specificity and transmission (8). Indeed, there is evidence through generation of both chimeric receptors and peptides to suggest that this is true for many family B receptors (9–16). However, there is also evidence that ligand recognition and affinity determination can rely on interaction with the receptor core (14, 17–24); this is particularly evident with the glucagon receptor, where changes in the N terminus of the glucagon peptide significantly alter its binding affinity at the glucagon receptor (17, 25, 26). In addition, sub-

* This work was supported in part by the National Health and Medical Research Council of Australia Project Grant 1002180 and Program Grant 519461 and by National Health and Medical Research Council Principal Research Fellowship (to P. M. S.) and a Senior Research Fellowship (to A. C.).
[S] This article contains supplemental Table S1 and Fig. S1.
[1] Senior Research Fellow of the National Health and Medical Research Council.
[2] Principal Research Fellow of the National Health and Medical Research Council. To whom correspondence should be addressed: Drug Discovery Biology, Monash Institute of Pharmaceutical Sciences, Monash University, 381 Royal Parade, Parkville, Victoria 3052, Australia. Tel.: 3-9903-9069; Fax: 3-9903-9581; E-mail: Patrick.Sexton@monash.edu.

[3] The abbreviations used are: GPCR, G protein-coupled receptor; ECL, extracellular loop; GLP-1R, glucagon-like peptide 1 receptor; Ca^{2+}_i, intracellular calcium; TM, transmembrane.

stitution of many N-terminal residues of the GLP-1, vasoactive intestinal polypeptide, and secretin peptides for alanine significantly reduce binding affinity at the GLP-1R, VPAC receptors, and secretin receptor, respectively (21, 23, 24), illustrating that effective ligand recognition, binding, and subsequent biological activity require the entire length of peptide and involve multiple domains within the receptor.

Although crystal and NMR structures have been resolved for the isolated N terminus of several ligand-bound family B GPCRs, including the gastric inhibitory polypeptide receptor (27), corticotrophin-releasing factor receptors (28–30), parathyroid hormone 1 receptor (31), and GLP-1 R (32, 33), only limited mutagenesis and photoaffinity labeling data are available to aid in understanding the role of core domain residues. Nevertheless, the data available highlight the significance of the receptor core region in both peptide binding and receptor activation (34, 35), including residues within the putative ECL2 of the GLP-1R (36, 37), secretin receptor (18), corticotrophin-releasing factor receptors (38, 39), and parathyroid hormone receptors (16), suggesting this potentially forms a significant site of interaction for the N-terminal amino acids of the peptide ligands and/or plays an important role in stabilizing active state conformations in the presence of ligand.

Like most GPCRs, family B receptors are promiscuously coupled, including pathway coupling that leads to cAMP signaling, $Ca^{2+}{}_i$ mobilization, and pERK1/2, each of which is linked to important physiological functions of the receptors (40–42). The relative activation of these signaling pathways may therefore be important for optimal development of therapeutics. Nonetheless, our mechanistic understanding of how family B receptors activate these distinct pathways is limited.

In this study, we explore the influence of individual ECL2 residues on human GLP-1R function. The GLP-1R is an important target in the development of therapeutics for type II diabetes mellitus, with actions including glucose-dependent increases in insulin biosynthesis and secretion, increasing β-cell mass, and decreasing body mass, all effects that address major symptoms of type II diabetes mellitus (43). Despite its therapeutic promise, relatively limited data are available on the contribution of domains in the receptor core on ligand binding and receptor activation. We have performed systematic substitution of each residue of ECL2 of the human GLP-1R by alanine and assessed the effects across a series of pharmacological outputs, which demonstrated critical residues for receptor activation that vary in an agonist peptide- or pathway-specific manner.

EXPERIMENTAL PROCEDURES

Materials—Dulbecco's modified Eagle's medium (DMEM), hygromycin-B, and Fluo-4 acetoxymethyl ester were purchased from Invitrogen. Fetal bovine serum (FBS) was purchased from Thermo Fisher Scientific (Melbourne, Victoria, Australia). The QuikChange™ site-directed mutagenesis kit was purchased from Stratagene (La Jolla, CA). AlphaScreen™ reagents, Bolton-Hunter reagent (^{125}I), and 384-well ProxiPlates were purchased from PerkinElmer Life Sciences. SureFire™ ERK1/2 reagents were generously supplied by TGR Biosciences (Adelaide, South Australia, Australia). Sigma*Fast o*-phenylenediamine dihydrochloride tablets and antibodies were purchased from Sigma. GLP-1 peptides were purchased from American Peptide (Sunnyvale, CA). All other reagents were purchased from Sigma or Merck and were of an analytical grade.

Receptor Mutagenesis—To study the influence of specific amino acids of ECL2 on receptor function, the desired mutations were introduced to an N-terminally double c-Myc-labeled wild type human GLP-1R in the pEF5/FRT/V5-DEST destination vector (Invitrogen); this receptor had equivalent pharmacology to the untagged human GLP-1R (data not shown). Mutagenesis was carried out using oligonucleotides for site-directed mutagenesis from GeneWorks (Hindmarsh, South Australia, Australia) (supplemental Table S1) and the QuikChange™ site-directed mutagenesis kit (Stratagene). Sequences of receptor clones were confirmed by cycle sequencing as described previously (44). Mutated residues and their conservation across human family B peptide hormone receptors are illustrated in Fig. 1.

Transfections and Cell Culture—Wild type and mutant human GLP-1R were isogenically integrated into FlpIn-Chinese hamster ovary (FlpInCHO) cells (Invitrogen) and selection of receptor-expressing cells accomplished by treatment with 600 μg ml^{-1} hygromycin-B as described previously (44). Transfected and parental FlpInCHO cells were maintained in DMEM supplemented with 10% heat-inactivated FBS and incubated in a humidified environment at 37 °C in 5% CO_2.

Radioligand Binding Assay—FlpInCHO wild type and mutant human GLP-1R cells were seeded at a density of 3×10^4 cells/well into 96-well culture plates and incubated overnight at 37 °C in 5% CO_2, and radioligand binding was carried out as described previously (45). For each cell line in all experiments, total binding was defined by 0.5 nM ^{125}I-exendin(9–39) alone, and nonspecific binding was defined by 1 μM exendin(9–39). For analysis, data are normalized to the B_0 value for each individual experiment.

cAMP Accumulation Assay—FlpInCHO wild type and mutant human GLP-1R cells were seeded at a density of 3×10^4 cells/well into 96-well culture plates and incubated overnight at 37 °C in 5% CO_2, and cAMP detection was carried out as described previously (46). All values were converted to concentration of cAMP using a cAMP standard curve performed in parallel, and data were subsequently normalized to the response of 100 μM forskolin in each cell line.

pERK1/2 Assay—FlpInCHO wild type and mutant human GLP-1R cells were seeded at a density of 3×10^4 cells/well into 96-well culture plates and incubated overnight at 37 °C in 5% CO_2. Receptor-mediated pERK1/2 was determined using the AlphaScreen™ ERK1/2 SureFire™ protocol as described previously (44). Initial pERK1/2 time course experiments were performed over 1 h to determine the time at which agonist-mediated pERK1/2 was maximal. Subsequent experiments were then performed at the time required to generate a maximal pERK1/2 response (6 min). Data were normalized to the maximal response elicited by 10% FBS in each cell line, determined at 6 min (peak FBS response).

$Ca^{2+}{}_i$ Mobilization Assay—FlpInCHO wild type and mutant human GLP-1R cells were seeded at a density of 3×10^4 cells/

well into 96-well culture plates and incubated overnight at 37 °C in 5% CO_2, and receptor-mediated $Ca^{2+}{}_i$ mobilization was determined as described previously (47). Fluorescence was determined immediately after peptide addition, with an excitation wavelength set to 485 nm and an emission wavelength set to 520 nm, and readings were taken every 1.36 s for 120 s. Peak magnitude was calculated using five-point smoothing, followed by correction against basal fluorescence. The peak value was used to create concentration-response curves. Data were normalized to the maximal response elicited by 100 μM ATP.

Cell Surface Receptor Expression—FlpInCHO wild type and mutant human GLP-1R cells, with receptor DNA previously incorporated with an N-terminal double c-Myc epitope label, were seeded at a density of 25×10^4 cells/well into 24-well culture plates and incubated overnight at 37 °C in 5% CO_2, washed three times in 1× PBS, and fixed with 3.7% paraformaldehyde at 4 °C for 15 min. Cell surface receptor detection was then performed as described previously (45). Data were normalized to the basal fluorescence detected in FlpInCHO parental cells. Specific ^{125}I-exendin(9–39) binding at each receptor mutant, as identification of functional receptors at the cell surface, was also determined (corrected for nonspecific binding using 1 μM exendin(9–39)).

Data Analysis—All data were analyzed using Prism 5.04 (GraphPad Software Inc., San Diego). For all analyses the data are unweighted, and each *y* value (mean of replicates for each individual experiment) is considered an individual point. Concentration response signaling data were analyzed using a three-parameter logistic equation as described previously (44) and as shown in Equation 1,

$$Y = \text{Bottom} + \frac{(\text{Top} - \text{Bottom})}{1 + 10^{(\log EC_{50} - \log[A])}} \quad \text{(Eq. 1)}$$

where Bottom represents the *y* value in the absence of ligand(s); Top represents the maximal stimulation in the presence of ligand(s); [*A*] is the molar concentration of ligand, and EC_{50} represents the molar concentration of ligand required to generate a response halfway between Top and Bottom. Similarly, Equation 1 was used in the analysis of inhibition binding data, instead replacing EC_{50} with IC_{50}. In this case, Bottom defines the specific binding of the radioligand that is equivalent to nonspecific ligand binding, whereas Top defines radioligand binding in the absence of a competing ligand, and the IC_{50} value represents the molar concentration of ligand required to generate a response halfway between Top and Bottom. IC_{50} values obtained were then corrected for radioligand occupancy as described previously (48) using the radioligand affinity (K_i) experimentally determined for each mutant.

To quantify efficacy in the system, all data were fitted with an operational model of agonism (49) as shown in Equation 2,

$$Y = \text{Bottom} + \frac{E_m - \text{Bottom}}{1 + ((10^{\log K_A}) + (10^{\log[A]}))/(10^{(\log\tau + \log[A])})} \quad \text{(Eq. 2)}$$

where Bottom represents the *y* value in the absence of ligand(s); E_m represents the maximal stimulation of the system; K_A is the agonist-receptor dissociation constant, in molar concentration; [*A*] is the molar concentration of ligand, and τ is the operational measure of efficacy in the system, which incorporates signaling efficacy and receptor density. Constraints for this model were determined by fitting the operational model for a partial agonist to each of the peptides at the wild type receptor, with the most efficacious peptide fitted with Equation 3,

$$Y = \text{Bottom} + \frac{E_m - \text{Bottom}}{1 + 10^{(\log EC_{50} - \log[A])}} \quad \text{(Eq. 3)}$$

and the less efficacious peptides were fitted with Equation 2, to obtain a value for the system maximum (E_m) at the wild type receptor. This value was then globally constrained in the operational model (Equation 2) when applied at each of the mutant receptors. All estimated τ values were then corrected to cell surface expression (τ_c) as determined by specific ^{125}I-exendin(9–39) binding, and errors were propagated from both τ and cell surface expression. Changes in τ_c with respect to wild type for each mutant were used to generate correlation plots, which were subsequently fitted with linear regression and outliers established at greater than three standard deviations from regression.

To quantify signaling bias, peptide agonist concentration-response curves were analyzed with nonlinear regression using an operational model of agonism (50), but modified to directly estimate the ratio of τ_c/K_A, in a manner similar to that described by Figueroa *et al.* (51). For each pathway, as shown in Equation 4,

$$Y = \frac{E_{max} \times (\tau_c/K_A)^n \times [A]^n}{[A]^n \times (\tau_c/K_A)^n + (1 + [A]/K_A)^n} \quad \text{(Eq. 4)}$$

the parameters are as defined for Equation 2. All estimated τ_c/K_A ratios included propagation of error for both τ_c and K_A. Changes in τ_c/K_A ratios with respect to wild type of each mutant were used to quantitate bias between signaling pathways. Accordingly, bias factors included propagation of error from τ_c/K_A ratios of each pathway.

Data were also normalized to maximal agonist response at the wild type receptor in each signaling pathway, fitted with a three-parameter logistic equation, and equimolar concentrations of agonists in each pathway plotted against one other. In this way, the bias of any given agonist for one pathway over another can be visualized (50). In all cases, individual data sets were unweighted during the analyses.

Statistics—Changes in peptide affinity, potency, efficacy, and cell surface expression of ECL2 mutants in comparison with wild type control were statistically analyzed with one-way analysis of variance and Dunnett's post test, and significance was accepted at $p < 0.05$.

RESULTS

Cell Surface Expression of Human GLP-1R ECL2 Alanine Mutants

Wild type c-Myc human GLP-1R and each of the human GLP-1R ECL2 alanine mutants (Fig. 1*A*) were isogenically integrated into FlpInCHO host cells by recombination, allowing the

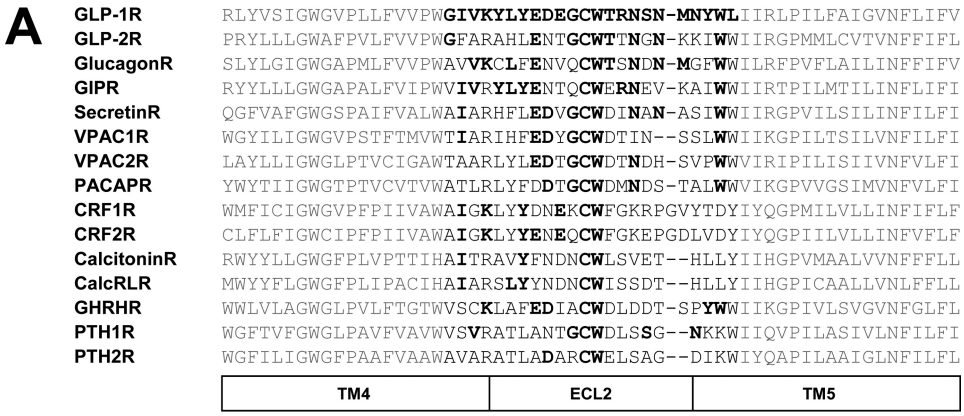

FIGURE 1. **Amino acid sequence alignments.** *A,* alignments of putative ECL2 of human family B GPCRs, with absolute conservation of residues with respect to human GLP-1R, are highlighted in *boldface*, and putative TM/ECL2 boundaries are indicated; *B,* human family B peptides, with absolute conservation of residues with respect to human GLP-1 peptide, are highlighted in *boldface*.

comparison of cell surface expression by antibody detection of the N-terminal double c-Myc epitope label without complications arising from variations in gene transcription. In this study, we observed total abolishment of cell surface receptor expression of the W306A mutant (Fig. 2*A* and Table 1). Significant increases in cell surface receptor antibody labeling were observed for the N300A and M303A mutants, although decreases were observed for D293A, C296A, W297A, S301A, N304A, Y305A, and L307A. No other mutant deviated significantly in cell surface receptor antibody labeling in comparison with wild type, although there were occasional trends for increases or decreases. In most cases, the changes in cell surface expression identified through antibody detection of the epitope label were consistent with the pattern of specific binding of ^{125}I-exendin(9–39) at each of the mutant receptors in comparison with wild type receptor, although generically the ^{125}I-exendin(9–39) binding trended lower for the mutants relative to the wild type, when compared with receptor antibody labeling (Fig. 2*B* and Table 1). Notable exceptions to this were E294A and T298A that demonstrated increased ^{125}I-exendin(9–39) binding but wild type levels of receptor antibody labeling and Y305A that displayed wild type levels of ^{125}I-exendin(9–39) binding and reduced antibody labeling. At each of these receptor mutants, the affinity of exendin(9–39) (determined through homologous competition binding) was not significantly different from the wild type receptor (Table 1). As exendin(9–39) affinity was unaltered at all mutant receptors, reductions in ^{125}I-exendin(9–39) binding but not antibody labeling may suggest a subpopulation of receptors for which the ligand binding domain of the receptor is misfolded, leading to loss of functional receptors at the cell surface. In these cases, however, antibody detection of the inserted epitope tag does not discriminate between different conformational states of the ligand binding domain and therefore has most likely detected all populations of receptor at the cell surface. The mechanism underlying high ^{125}I-exendin(9–39) in the absence of changes to antibody labeling is less clear but may be due to altered conformation of the c-Myc epitope or an increase in the relative proportion of receptors in an inactive state.

Select Mutants of the Human GLP-1R ECL2 Influence GLP-1(7–36)-NH$_2$ Binding Affinity but Not Exendin(9–39) Affinity

To establish the binding profiles of each of the human GLP-1R ECL2 alanine mutants, equilibrium binding studies were performed with the endogenous peptide agonists GLP-1(1–36)-NH$_2$ and GLP-1(7–36)-NH$_2$ in competition with the radiolabeled orthosteric antagonist, ^{125}I-exendin(9–39). There was no significant deviation in antagonist exendin(9–39) affinity at any of the mutated ECL2 residues, with the exception of the W306A mutant, where no value could be defined as it was undetectable at the cell surface (Table 1).

Full inhibition curves for the GLP-1(1–36)-NH$_2$ peptide could not be established over the concentration range tested; at the highest concentration assayed (1 μM), the level of binding inhibition for most of the mutants was not significantly different from wild type receptor (Fig. 3, *A* and *B*). However, no clear

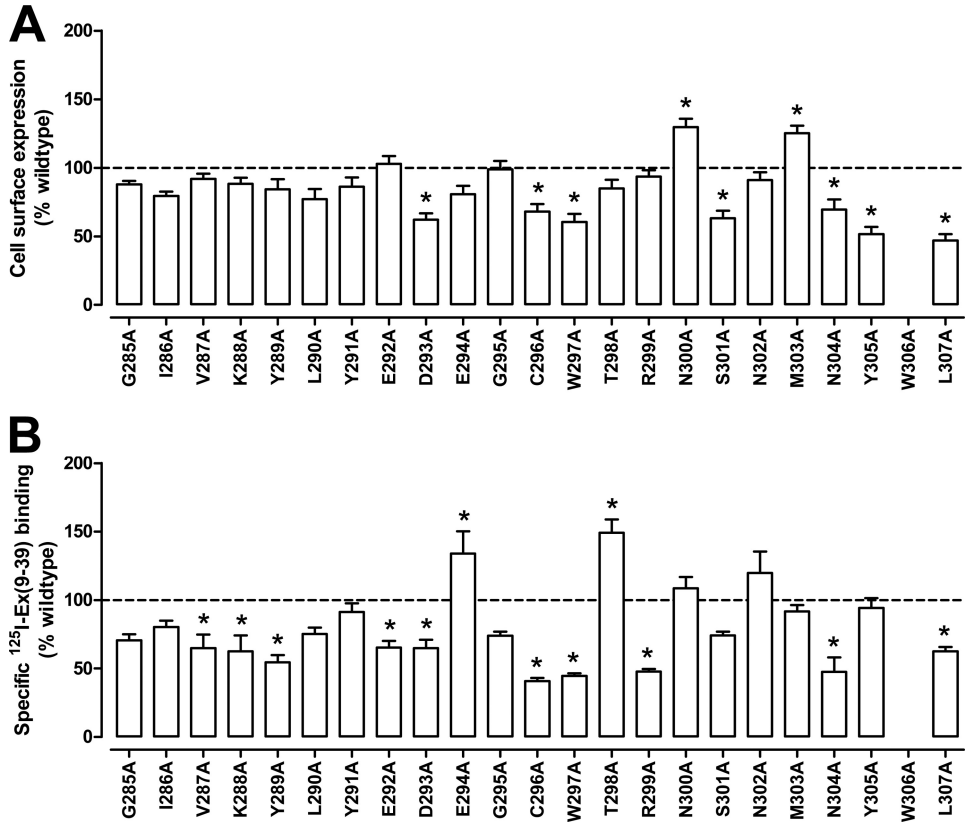

FIGURE 2. **Cell surface expression profiles of human GLP-1R ECL2 alanine mutants.** Cell surface expression profiles of each of the human GLP-1R ECL2 alanine mutants are compared with wild type stably transfected into FlpInCHO cells as determined through antibody detection of the N-terminal c-Myc epitope label (*A*) and by specific ^{125}I-exendin(9–39) binding (*B*). Statistical significance of changes in total cell surface expression in comparison with wild type human GLP-1R expression (100%) was determined by one-way analysis of variance and Dunnett's post-test and are indicated with an *asterisk* (*, $p < 0.05$). All data are means ± S.E. of seven to nine or three to four independent experiments conducted in duplicate for antibody detection and specific ^{125}I-exendin(9–39) binding, respectively.

effect on binding was observed for C296A, W297A, R299A, and Y305A (Fig. 3, *A* and *B*). This was likely a result of the poor radioligand binding window for these mutants arising from the low specific ^{125}I-exendin(9–39) binding (Table 1).

There were no significant changes in affinity of GLP-1(7–36)-NH_2 in comparison with the wild type control for G285A, I286A, V287A, Y289A, L290A, Y291A, E294A, G295A, T298A, S301A, and N304A (Table 1). Decreases in binding affinity of GLP-1(7–36)-NH_2 in comparison with wild type were observed for K288A, E292A, D293A, R299A, N300A, N302A, M303A, Y305A, and L307A mutants, as highlighted by gray shading in Table 1 (Fig. 3, *C* and *D*, and Table 1).

Effect of Human GLP-1R ECL2 Alanine Mutations on Peptide-mediated cAMP Accumulation

Binding Affinity-modified Mutants—There was no measurable GLP-1(1–36)-NH_2-mediated cAMP response at the K288A, E292A, C296A, W297A or N300A mutants, and significant depression in E_{max} was observed at the D293A, R299A, N302A, M303A, Y305A, and L307A mutants (Fig. 4*A* and Table 2). Application of the operational model indicated that each of these mutant receptors had a significantly reduced coupling efficiency for cAMP, after correction for functional cell surface receptor levels (Fig. 4, *A* and *E*, and Table 2). Throughout the results, the operational measure of efficacy (τ_c) is used as the principal measure of changes in efficacy for each pathway, as this accounts for both alterations in coupling efficiency and cell surface receptor expression (50).

All mutants displaying significantly decreased GLP-1(7–36)-NH_2 binding affinity (K288A, E292A, D293A, C296A, W297A, R299A, N300A, N302A, M303A, Y305A, and L307A) also exhibited reduced potency for cAMP in response to this peptide, although this was not significant for the M303A mutant (Fig. 4*B* and Table 2). Assessment of the effect on efficacy indicated that all mutants also had diminished coupling efficiency in addition to decreased affinity, although this effect was minimal for D293A, C296A, and Y305A, where statistical significance was not reached (Fig. 4, *B* and *F*, and Table 2). Not surprisingly, cells expressing the W306A mutant did not respond to peptide stimulation (Table 2).

Mutants with Unaltered Binding Affinity—For mutants that were not affected at the level of peptide agonist binding, potency was mostly unaltered with two exceptions as follows: the V287A mutant, where decreased potency of GLP-1(7–36)-NH_2 was observed, and the T298A mutant that had increased potency of GLP-1(7–36)-NH_2 (Fig. 4*D* and Table 2). For the latter, the increased potency was paralleled by higher expression of functional cell surface receptors (Fig. 1*B*) but was accompanied by reduced efficacy (Fig. 4*F* and Table 2). Interestingly, the loss of potency at the V287A mutant occurred in the absence of significant changes in efficacy, for either the

TABLE 1

Effects of human GLP-1R ECL2 alanine mutants on peptide ligand binding and cell surface expression

Binding data were analyzed using a three-parameter logistic equation as defined in Equation 1 to obtain pIC_{50} values. pIC_{50} values were then corrected for radioligand occupancy using the radioligand dissociation constant for each mutant, allowing determination of ligand affinity (K_i). Data are normalized to maximum ^{125}I-exendin(9–39) binding in the absence of ligand, with nonspecific binding measured in the presence of 1 μM exendin(9–39). For specific ^{125}I-exendin(9–39) binding, data are expressed as a maximum of specific ^{125}I-exendin(9–39) binding at the wild type human GLP-1R. Cell surface expression was determined through antibody detection of the N-terminal c-Myc epitope label, with data expressed as a maximum of wild type human GLP-1R expression. All values are expressed as means ± S.E. of three to four (binding) or seven to nine (cell surface expression) independent experiments, conducted in duplicate. Data were analyzed with one-way analysis of variance and Dunnett's post test. Gray shading highlights residues effecting peptide agonist binding affinity. ND means data were unable to be experimentally defined.

	Binding (pK_i)**		Cell surface expression (% wildtype)	Specific ^{125}I-exendin(9-39) binding (% wildtype)
	GLP-1(7-36)NH_2	Exendin(9-39)		
Wildtype	8.7 ± 0.1	7.7 ± 0.1	100 ± 5	100 ± 2
G285A	9.1 ± 0.1	7.7 ± 0.1	88 ± 3	70 ± 4
I286A	8.8 ± 0.1	7.7 ± 0.2	79 ± 3	80 ± 5
V287A	8.5 ± 0.1	7.7 ± 0.1	92 ± 4	**65 ± 10***
K288A	**6.6 ± 0.3***	8.0 ± 0.1	88 ± 5	**62 ± 12***
Y289A	8.9 ± 0.1	7.6 ± 0.2	84 ± 7	**55 ± 5***
L290A	8.3 ± 0.1	7.7 ± 0.1	77 ± 7	75 ± 5
Y291A	8.3 ± 0.1	7.8 ± 0.1	86 ± 7	91 ± 7
E292A	**6.7 ± 0.2***	7.7 ± 0.1	103 ± 6	**65 ± 5***
D293A	**7.3 ± 0.1***	7.9 ± 0.1	**62 ± 5***	**65 ± 6***
E294A	8.8 ± 0.1	8.0 ± 0.1	81 ± 6	**134 ± 16***
G295A	8.7 ± 0.1	7.7 ± 0.1	99 ± 6	74 ± 3
C296A	**7.6 ± 0.4***	7.8 ± 0.2	**68 ± 5***	**41 ± 2***
W297A	**6.9 ± 0.5***	7.9 ± 0.2	**60 ± 6***	**45 ± 2***
T298A	9.1 ± 0.1	8.1 ± 0.1	85 ± 6	**149 ± 10***
R299A	**7.2 ± 0.4***	7.4 ± 0.2	94 ± 5	**48 ± 2***
N300A	**6.6 ± 0.2***	7.9 ± 0.1	**130 ± 6***	109 ± 8
S301A	8.8 ± 0.1	8.1 ± 0.1	**63 ± 5***	74 ± 3
N302A	**7.3 ± 0.1***	8.0 ± 0.1	91 ± 6	120 ± 16
M303A	**8.1 ± 0.1***	8.1 ± 0.1	**125 ± 5***	92 ± 5
N304A	8.4 ± 0.3	7.5 ± 0.2	**70 ± 7***	**48 ± 10***
Y305A†	**6.8 ± 0.2***	7.7 ± 0.1	**52 ± 5***	94 ± 7
W306A†	**N.D.**	**N.D.**	**N.D.**	**N.D.**
L307A	**7.6 ± 0.2***	8.0 ± 0.1	**47 ± 5***	**63 ± 3***

* Data are statistically significant at $p < 0.05$, one-way analysis of variance, and Dunnett's post test in comparison with wild type response.

** R^2 values for the curve fits were all >0.5, except for GLP-1(7–36)-NH_2 at the W297A ($R^2 = 0.42$) and R299A ($R^2 = 0.46$) mutants.

† GLP-1(1–36)-NH_2 binding profile deviates from wild type, but the pIC_{50} value for this ligand was unable to be determined in the concentration range tested.

full-length or truncated peptide. Overall, similar effects on efficacy were observed for GLP-1(1–36)-NH_2 and GLP-1(7–36)-NH_2 across the ECL2 mutants (Fig. 4, *E* and *F*, and Table 2). G285A, I286A, V287A, and Y289A, located at the top of TM4/proximal ECL2, had minimal effects on the efficacy of both peptides. Similarly, there was little effect on cAMP efficacy with the G295A mutant. All other mutants displayed loss of efficacy for both peptides, although the effect was not always significant for both peptides. For example, there was a greater effect on GLP-1(1–36)-NH_2 efficacy with the L290A mutant and a greater effect on GLP-1(7–36)-NH_2 efficacy for the E294A, T298A, and S301A mutants. For both peptides, the greatest decrease in efficacy was seen with the N304A mutant (Table 2).

Effect of Human GLP-1R ECL2 Alanine Mutations on Peptide-mediated pERK1/2

Binding Affinity-modified Mutants—Peptide-induced pERK1/2 was determined at 6 min for each of the human GLP-1R ECL2 alanine mutants. Consistent with cAMP accumulation, there were no statistically significant differences in GLP-1(1–36)-NH_2 potency at these mutant receptors, although no measurable response was seen for either N300A or W306A (Fig. 5*A* and Table 3). In general, there was less impact of the ECL2 mutants on GLP-1(1–36)-NH_2-mediated pERK1/2 signaling relative to effects on cAMP response. Whereas the K288A, E292A, C296A, W297A, and N300A all lacked measurable cAMP responses in the presence of GLP-1(1–36)-NH_2, only the N300A mutant also failed to yield a pERK1/2 signal (Tables 2 and 3). Operational modeling of the effect of mutation on peptide efficacy failed to identify any significant changes for these mutants, although most trended toward lower efficacy (Fig. 5, *A* and *E*, and Table 3). The exception to this was R299A that trended higher in efficacy for pERK1/2 (Table 3).

As with the GLP-1(1–36)-NH_2 responses, there was generally less impact of ECL2 mutation on GLP-1(7–36)-NH_2-mediated pERK1/2 responses relative to the cAMP response (Fig. 5*B* and Tables 2 and 3). Potency was largely unaffected with only the K288A mutant exhibiting significantly lower potency, although there was a trend toward lower potency with some of the other affinity altered mutants, including E292A and C296A (Fig. 5, *B* and *F*, and Table 3). The greatest effects on GLP-1(7–36)-NH_2 efficacy were seen with E292A and N300A, the former being significantly lower (Fig. 5*F* and Table 3). K288A, D293A, W297A, N302A, Y305A, and L307A also trended toward lower efficacy. In contrast, C296A, R299A, and M303A displayed higher efficacy than the wild type receptor, although these effects did not reach significance. Interestingly, the effect on coupling efficiency of GLP-1(1–36)-NH_2 and GLP-1(7–36)-NH_2 was opposite for C296A and M303A suggesting that there are ligand-dependent effects imparted by these mutations (Table 3). Intriguingly, the R299A mutant displayed consistent effects for the two peptides but distinct effects in cAMP (decreased efficacy) *versus* pERK1/2 signaling (increased efficacy), suggesting a pathway selective role for this residue (Tables 2 and 3).

Mutants with Unaltered Binding Affinity—Overall, there was only limited impact of ECL2 mutants on the pERK1/2 responses for mutant receptors that had unaltered agonist binding affinity, and indeed, none of the effects achieved statistical significance for either GLP-1(1–36)-NH_2 or GLP-1(7–36)-NH_2 (Fig. 5, *C* and *D*, and Table 3). Nonetheless, there was further distinction in the pattern of pERK1/2 efficacy changes relative to $Ca^{2+}{}_i$ and cAMP signaling in that efficacy tended to increase for many of the mutants, including G285A, I286A, V287A, Y289A, G295A, and T298A in comparison with wild type (Fig. 5, *C–F*, and Table 3). The L290A and Y291A mutants tended to have decreased efficacy for the GLP-1(7–36)-NH_2 peptide but had little effect on GLP-1(1–36)-NH_2 responses. In contrast, N304A had an apparent increase in efficacy for GLP-1(1–36)-NH_2 but unaltered GLP-1(7–36)-NH_2 response (Table 3).

Effect of Human GLP-1R ECL2 Alanine Mutations on Peptide-mediated $Ca^{2+}{}_i$ Mobilization

Binding Affinity-modified Mutants—Consistent with previous data (46), there was no $Ca^{2+}{}_i$ response with full-length

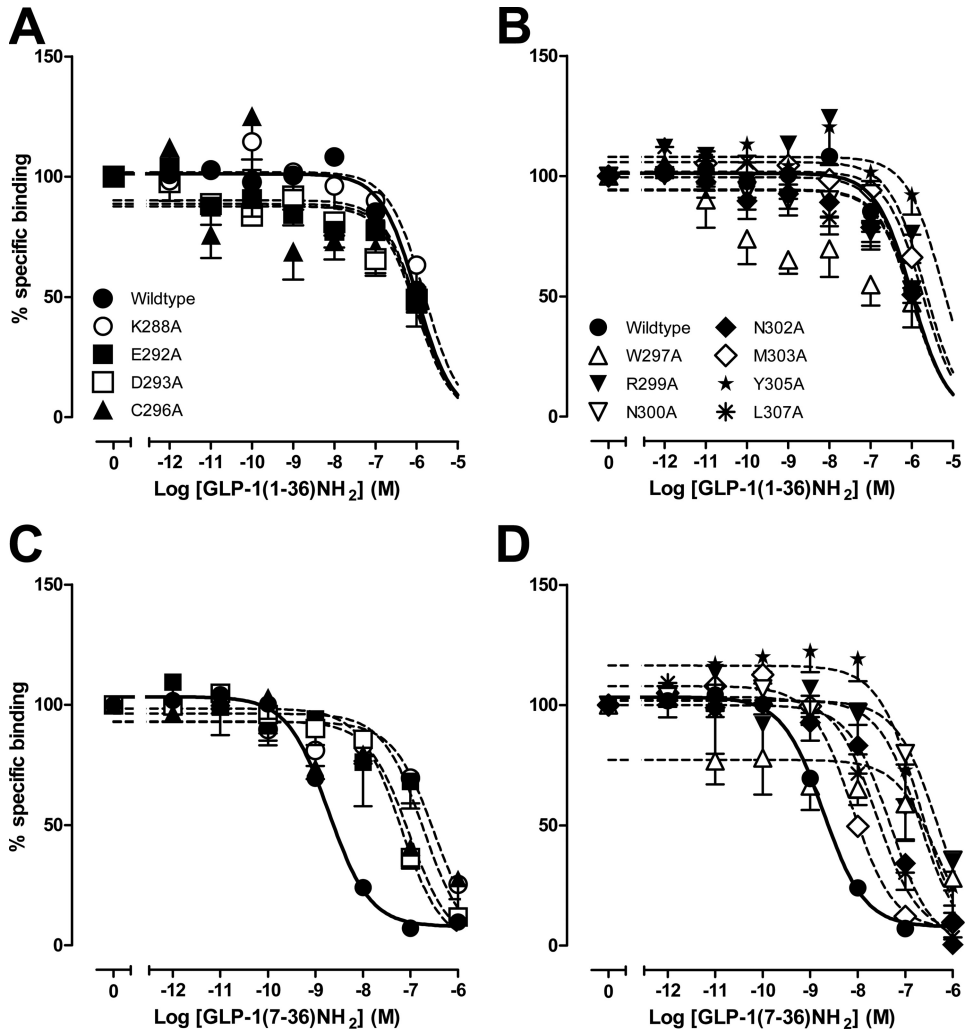

FIGURE 3. **Agonist binding profiles of human GLP-1R ECL2 alanine mutants.** Characterization of the binding of GLP-1(1–36)-NH_2 (*A* and *B*) and GLP-1(7–36)-NH_2 (*C* and *D*) in competition with the radiolabeled antagonist, ^{125}I-exendin(9–39), in whole FlpInCHO cells stably expressing the wild type human GLP-1R or each of the human GLP-1R ECL2 alanine mutants. Data are normalized to maximum ^{125}I-exendin(9–39) binding, with nonspecific binding measured in the presence of 1 μM exendin(9–39) and analyzed with a three-parameter logistic equation as defined in Equation 1. All values are means ± S.E. of three to four independent experiments, conducted in duplicate.

GLP-1 at either the wild type receptor or any of the alanine mutants (data not shown).

Mutants that displayed reduced GLP-1(7–36)-NH_2 binding affinity (K288A, E292A, D293A, C296A, W297A, R299A, N300A, N302A, M303A, Y305A, and L307A) displayed either significantly reduced $Ca^{2+}{}_i$ signaling or complete loss of signaling (Fig. 6*A* and Table 4). Notably, receptors with abolished $Ca^{2+}{}_i$ signaling (K288A, E292A, C296A, W297A, and N300A) were those that had the weakest ability to couple to the cAMP pathway, with the exception of C296A (Table 2). In addition, these mutants also had weak coupling to the pERK1/2 pathway, with the exception of C296A and W297A (Table 3). Dramatic reductions in GLP-1(7–36)-NH_2 efficacy were observed at the remaining affinity-affected mutant receptors D293A, R299A, N302A, M303A, Y305A, and L307A (Fig. 6, *A* and *C*, and Table 4). These decreases in ability to couple to the $Ca^{2+}{}_i$ pathway were mostly reflected in cAMP responses, although the extent of reductions in efficacy was in some cases inconsistent; D293A and Y305A were the most affected mutants in $Ca^{2+}{}_i$ but the least affected in cAMP coupling in the presence of GLP-1(7–36)-NH_2 (Tables 2 and 4). Generically, the decreases in $Ca^{2+}{}_i$ coupling were also reflected in pERK1/2 pathway coupling, with the exception of R299A and M303A (Tables 3 and 4).

Mutants with Unaltered Binding Affinity—All mutants had reduced GLP-1(7–36)-NH_2 efficacy relative to the wild type receptor, although the effect was not significant for G285A, I286A, V287A, L290A, G295A, and S301A that were among the least affected with respect to cAMP response (Fig. 6, *B* and *C*, and Table 4). For nonbinding affected mutants, the greatest effect on efficacy was observed with the N304A mutant, again consistent with the magnitude of effect on cAMP signaling (Tables 2 and 4).

Effect of Human GLP-1R ECL2 Alanine Mutations on Peptide-mediated Signal Bias

As noted previously (46), GLP-1(1–36)-NH_2 exhibits distinct signal bias to that evoked by GLP-1(7–36)-NH_2. GLP-1(7–36)-NH_2 is strongly biased toward cAMP formation relative to either pERK1/2 or $Ca^{2+}{}_i$ mobilization (supplemental Fig. S1, *B* and *C*). In

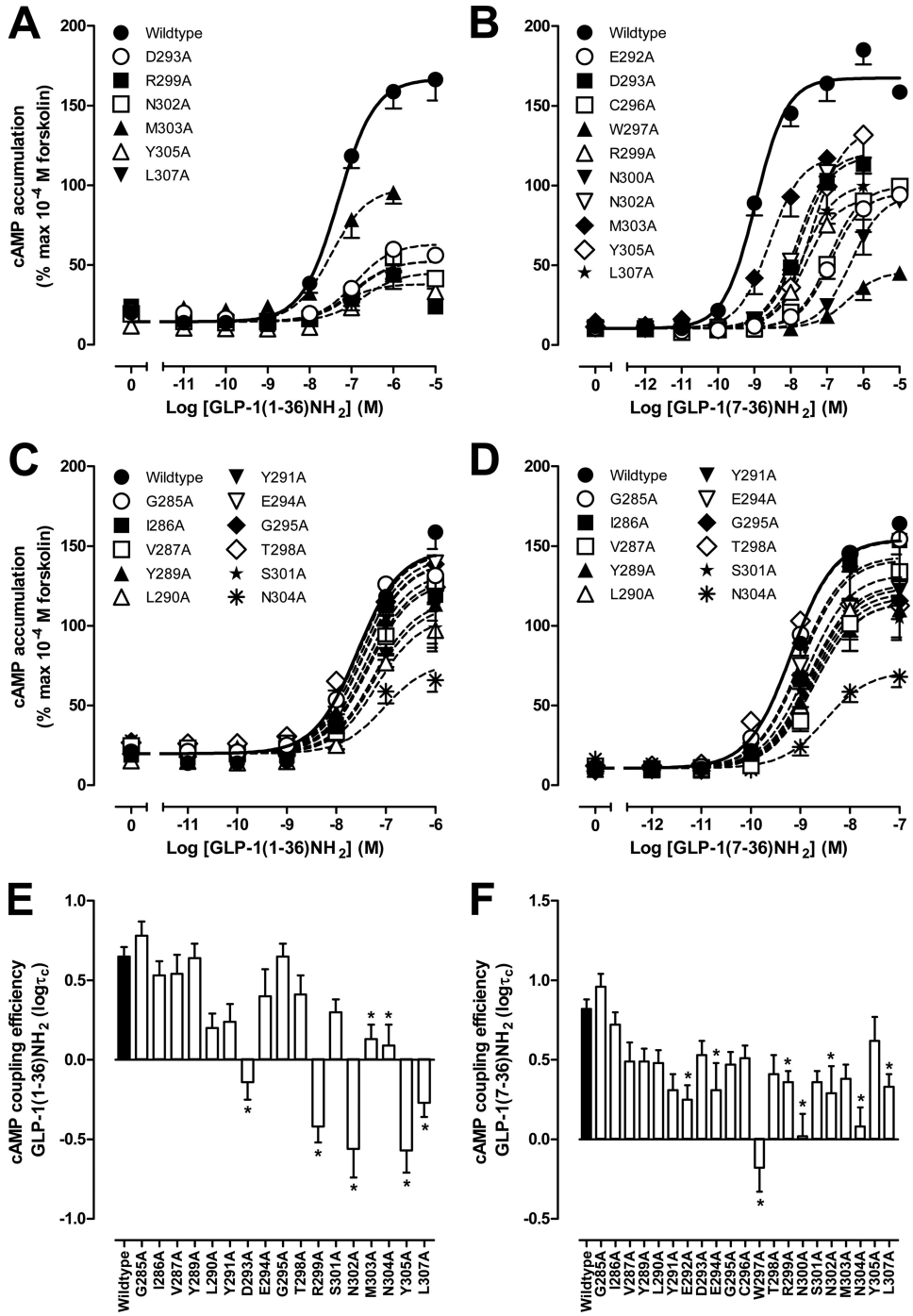

FIGURE 4. **cAMP accumulation profiles of human GLP-1R ECL2 alanine mutants.** Characterization of cAMP accumulation in the presence of GLP-1(1–36)-NH_2 (*A* and *C*) and GLP-1(7–36)-NH_2 (*B* and *D*) in FlpInCHO cells stably expressing the wild type human GLP-1R or each of the human GLP-1R ECL2 alanine mutants that effect peptide binding affinity (*A* and *B*) or has no significant effect on peptide binding affinity (*C* and *D*) is shown. Data are normalized to the response elicited by 100 μM forskolin and analyzed with an operational model of agonism as defined in Equation 2. All values are means ± S.E. of four to seven independent experiments, conducted in duplicate. Visual representation of cAMP pathway coupling efficacy (logτ_c) in the presence of GLP-1(1–36)-NH_2 (*E*) GLP-1(7–36)-NH_2 and (*F*) is shown. Statistical significance of changes in coupling efficacy in comparison with wild type human GLP-1R was determined by one-way analysis of variance and Dunnett's post-test and is indicated with an *asterisk* (*, $p < 0.05$). All values are logτ_c ± S.E of four to seven independent experiments, conducted in duplicate.

contrast, GLP-1(1–36)-NH_2 has equivalent preference for cAMP and pERK1/2 (supplemental Fig. S1*A*). GLP-1(7–36)-NH_2, however, has only weak bias for the pERK1/2 pathway relative to $Ca^{2+}{}_i$ mobilization (supplemental Fig. S1*D*). As the GLP-1(1–36)-NH_2 peptide did not elicit an $Ca^{2+}{}_i$ response, relative bias against this pathway could not be determined. Nonetheless, the absence of response is indicative of bias toward cAMP and pERK1/2.

Bias plots provide a convenient visual representation of relative pathway response that is independent of absolute potency (50), although bias factors are a quantitative measure of changes to pathway bias, relative to the wild type receptor (50).

TABLE 2

Effects of human GLP-1R ECL2 alanine mutants on peptide agonist signaling via cAMP

Data were analyzed using a three-parameter logistic equation as defined in Equation 1. pEC_{50} values represent the negative logarithm of the concentration of agonist that produces half the maximal response. E_{max} represents the maximal response normalized to that elicited by 100 μM forskolin. All mutants were analyzed with an operational model of agonism (Equation 2) to determine logτ values. All logτ values were then corrected to specific ^{125}I-exendin(9–39) binding (logτ_c). Values are expressed as mean ± S.E. of four to seven independent experiments, conducted in duplicate. Data were analyzed with one-way analysis of variance and Dunnett's post test. Gray shading highlights residues effecting peptide agonist binding affinity. ND means data were unable to be experimentally defined. R^2 values for the global curve fits were 0.88 for GLP-1(7–36)-NH_2 and 0.92 for GLP-1(1–36)-NH_2, respectively.

	cAMP accumulation					
	GLP-1(1-36)NH_2			GLP-1(7-36)NH_2		
	pEC_{50}	E_{max}	logτ_c (τ_c)	pEC_{50}	E_{max}	logτ_c (τ_c)
Wildtype	7.3 ± 0.1	166.7 ± 5.3	0.65 ± 0.06 (4.47)	9.0 ± 0.1	167.4 ± 4.6	0.82 ± 0.06 (6.61)
G285A	7.7 ± 0.2	**139.1 ± 9.7***	0.78 ± 0.09 (6.03)	9.1 ± 0.1	155.2 ± 4.9	0.96 ± 0.08 (9.12)
I286A	7.6 ± 0.2	**127.7 ± 9.2***	0.53 ± 0.09 (3.39)	8.8 ± 0.2	156.8 ± 10.2	0.72 ± 0.08 (5.25)
V287A	7.2 ± 0.2	**134.4 ± 10.4***	0.54 ± 0.12 (3.47)	**8.4 ± 0.1***	**137.3 ± 7.0***	0.49 ± 0.12 (3.09)
K288A	**N.D.**	**N.D.**	**N.D.**	**N.D.**	**N.D.**	**N.D.**
Y289A	7.6 ± 0.3	**119.3 ± 12.9***	0.64 ± 0.09 (4.37)	8.9 ± 0.2	**110.9 ± 6.9***	0.49 ± 0.08 (3.09)
L290A	7.3 ± 0.1	**102.6 ± 5.1***	0.20 ± 0.09 (1.58)	8.7 ± 0.1	**134.1 ± 7.1***	0.48 ± 0.08 (3.02)
Y291A	7.2 ± 0.1	**119.3 ± 6.8***	0.24 ± 0.11 (1.74)	8.6 ± 0.1	**126.9 ± 5.9***	0.31 ± 0.10 (2.04)
E292A	**N.D.**	**N.D.**	**N.D.**	**6.9 ± 0.1***	**94.9 ± 5.4***	**0.25 ± 0.09 (1.78)***
D293A	6.8 ± 0.3	**64.1 ± 6.7***	**-0.14 ± 0.11 (0.72)***	**7.8 ± 0.1***	**118.0 ± 3.8***	0.53 ± 0.09 (3.39)
E294A	7.4 ± 0.1	144.3 ± 7.3	0.40 ± 0.17 (2.51)	9.1 ± 0.1	**122.5 ± 4.5***	**0.31 ± 0.17 (2.04)***
G295A	7.4 ± 0.1	145.7 ± 5.1	0.65 ± 0.08 (4.47)	9.1 ± 0.0	**113.6 ± 1.9***	0.47 ± 0.08 (2.95)
C296A	**N.D.**	**N.D.**	**N.D.**	**6.9 ± 0.0***	**99.4 ± 2.7***	0.51 ± 0.08 (3.24)
W297A	**N.D.**	**N.D.**	**N.D.**	**6.5 ± 0.1***	**45.4 ± 3.6***	**-0.18 ± 0.15 (0.66)***
T298A	7.8 ± 0.1	**126.9 ± 5.3***	0.41 ± 0.12 (2.57)	**9.7 ± 0.1***	**116.2 ± 5.3***	0.41 ± 0.12 (2.57)
R299A	7.2 ± 0.5	**15.6 ± 2.8***	**-0.42 ± 0.10 (0.38)***	**7.6 ± 0.1***	**92.4 ± 4.1***	**0.36 ± 0.07 (2.29)***
N300A	**N.D.**	**N.D.**	**N.D.**	**6.3 ± 0.1***	**94.5 ± 6.1***	**0.02 ± 0.14 (1.05)***
S301A	7.5 ± 0.2	**102.9 ± 6.5***	0.30 ± 0.08 (2.00)	9.0 ± 0.2	**105.9 ± 6.5***	0.36 ± 0.07 (2.29)
N302A	7.0 ± 0.3	**52.4 ± 5.4***	**-0.56 ± 0.18 (0.28)***	**7.8 ± 0.1***	**120.3 ± 5.9***	**0.29 ± 0.17 (1.95)***
M303A	7.3 ± 0.2	**100.3 ± 6.4***	**0.13 ± 0.09 (1.35)***	8.5 ± 0.2	**119.1 ± 7.5***	0.38 ± 0.09 (2.40)
N304A	7.4 ± 0.3	**69.5 ± 6.0***	**0.09 ± 0.13 (1.23)***	8.5 ± 0.2	**71.2 ± 4.8***	**0.08 ± 0.12 (1.20)***
Y305A	6.9 ± 0.2	**44.9 ± 3.6***	**-0.57 ± 0.14 (0.27)***	**7.4 ± 0.2***	**136.0 ± 11.8***	0.62 ± 0.15 (4.17)
W306A	**N.D.**	**N.D.**	**N.D.**	**N.D.**	**N.D.**	**N.D.**
L307A	7.0 ± 0.2	**52.4 ± 3.9***	**-0.27 ± 0.09 (0.54)***	**7.6 ± 0.1***	**101.0 ± 4.9***	**0.33 ± 0.08 (2.14)***

* Data were statistically significant at $p < 0.05$, one-way analysis of variance and Dunnett's post test in comparison with the wild type response.

Comparison of all mutants in this manner indicates that most ECL2 mutants engender at least subtle changes to receptor bias, although residues Gly-285 and Ile-286 at the top of TM4 are exceptions to this (supplemental Fig. S1). The G285A mutation is interesting in that it engenders efficacy improvements for cAMP and pERK1/2 responses and was minimally altered with respect to $Ca^{2+}{}_i$ signaling. The mutants with the most dramatic effects on relative signal bias were also those that were altered in binding affinity of GLP-1(7–36)-NH_2, with the exception of N304A, which consistently had a large differential effect across pathways, and the T298A mutant that was among those mutants with greatest effect on pERK1/2/cAMP for GLP-1(1–36)-NH_2 and for $Ca^{2+}{}_i$/pERK1/2 for GLP-1(7–36)-NH_2 (supplemental Fig. S1, *A* and *D*), although the effect of these mutants was not significant in bias factor calculations (Table 5). Bias of cAMP or pERK1/2 relative to $Ca^{2+}{}_i$ was only moderately affected by most mutants (supplemental Fig. S1, *C* and *D*); the principal effect for $Ca^{2+}{}_i$/cAMP for GLP-1(7–36)-NH_2 was a loss of efficacy for cAMP production rather than alteration to bias *per se*, and this is reflected in the generally small changes to bias factors for these pathways (Table 5). This is probably not surprising as $Ca^{2+}{}_i$ is the weakest coupled pathway at the wild type receptor, as discussed above. The greatest effects on bias were seen with specific mutants on pERK1/2/cAMP profiles (supplemental Fig. S1, *A* and *B*; Table 5). This was evident as preservation of pERK1/2 response with near abolition of cAMP response for R299A, N302A, N304A, and Y305A for GLP-1(1–36)-NH_2 and a complete reversal of bias for GLP-1(7–36)-NH_2 such that pERK1/2 was favored over cAMP for N300A, W297A, C296A, and R299A. There was no clear bias for E292A, N302A, N304A, and L307A, indicating loss of the cAMP bias seen with the wild type receptor.

The effect of mutations to both increase and decrease efficacy of ERK1/2 activation likely reflects the divergent pathways that link receptor activation to pERK1/2, including both G protein-independent (52–55) and G protein-dependent mechanisms (56). It is interesting to note that the most profound differential effects on signaling occur with mutation to residues distal to, or including, the conserved Cys-296/Trp-297 motif. This segment of ECL2 is also the most important with respect to binding of small molecule ligands into the TM region of family A GPCRs (57–61).

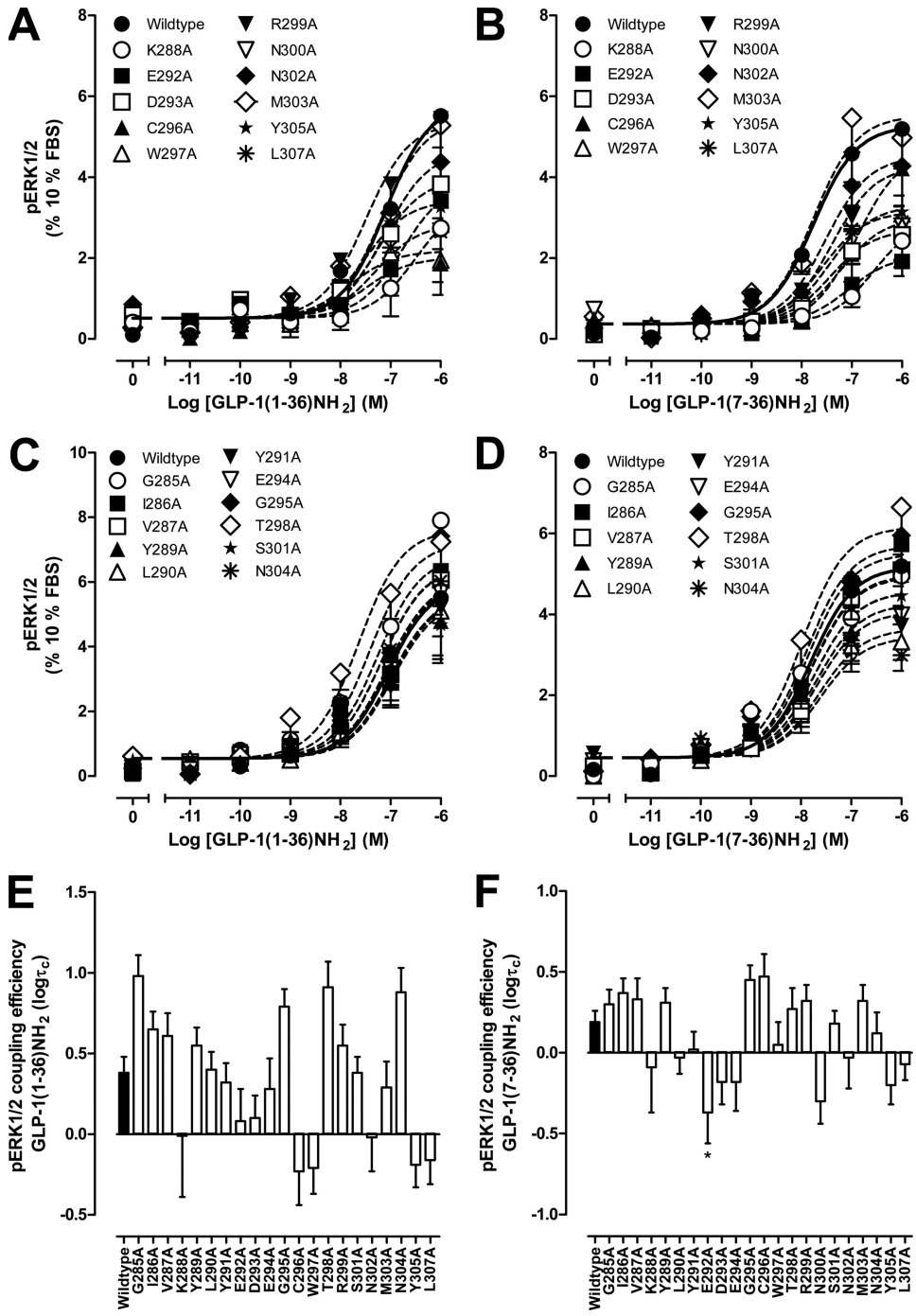

FIGURE 5. **pERK1/2 profiles of human GLP-1R ECL2 alanine mutants.** Characterization of pERK1/2 in the presence of GLP-1(1–36)-NH_2 (*A* and *C*) and GLP-1(7–36)-NH_2 (*B* and *D*) in FlpInCHO cells stably expressing the wild type human GLP-1R or each of the human GLP-1R ECL2 alanine mutants that effect peptide binding affinity (*A* and *B*) or has no significant effect on peptide binding affinity (*C* and *D*) is shown. Data are normalized to the maximal response elicited by 10% FBS and analyzed with an operational model of agonism as defined in Equation 2. All values are means ± S.E. of five to seven independent experiments, conducted in duplicate. Visual representation of ERK1/2 coupling efficacy ($\log\tau_c$) in the presence of GLP-1(1–36)-NH_2 (*E*) and GLP-1(7–36)-NH_2 (*F*). Statistical significance of changes in coupling efficacy in comparison with wild type human GLP-1R was determined by one-way analysis of variance and Dunnett's post-test and is indicated with an *asterisk* (*, $p < 0.05$). All values are $\log\tau_c$ ± S.E. five to seven independent experiments, conducted in duplicate.

DISCUSSION

It is widely accepted that the ECLs of family A GPCRs, particularly ECL2, are an important component for receptor function, with roles that include facilitating ligand binding, receptor trafficking, communication of ligand signal, and/or stabilization of an active ligand-receptor complex. Indeed, there is a plethora of evidence for many of these features (62–66), including the activation of rhodopsin relying on the displacement of the β-hairpin forming ECL2 via TM movement to allow ligand binding (67), the design of antibodies against ECL2 of several GPCRs that initiate a functional response (68, 69), and the substitution of several domains in the ECL2 of the human gonadotropin-releasing hormone receptor converting the activity of an antagonist to an agonist (70).

TABLE 3

Effects of human GLP-1R ECL2 alanine mutants on peptide agonist signaling via pERK1/2

Data were analyzed using a three-parameter logistic equation as defined in Equation 1. pEC_{50} values represent the negative logarithm of the concentration of agonist that produces half the maximal response. E_{max} represents the maximal response normalized to that elicited by 10% FBS. All mutants were analyzed with an operational model of agonism (Equation 2) to determine $\log\tau$ values. All $\log\tau$ values were then corrected to specific ^{125}I-exendin(9–39) binding ($\log\tau_c$). Values are expressed as means ± S.E. of five to seven independent experiments, conducted in duplicate. Data were analyzed with one-way analysis of variance and Dunnett's post test. R^2 values for the global curve fits were 0.68 for GLP-1(7–36)-NH_2 and 0.57 for GLP-1(1–36)-NH_2, respectively. Gray shading highlights residues effecting peptide agonist binding affinity. ND means data were unable to be experimentally defined.

	pERK1/2					
	GLP-1(1-36)NH_2			GLP-1(7-36)NH_2		
	pEC_{50}	E_{max}	$\log\tau_c$ (τ_c)	pEC_{50}	E_{max}	$\log\tau_c$ (τ_c)
Wildtype	7.2 ± 0.2	5.7 ± 0.5	0.38 ± 0.10 (2.40)	7.8 ± 0.2	5.3 ± 0.4	0.19 ± 0.07 (1.55)
G285A	7.1 ± 0.1	8.3 ± 0.6	0.98 ± 0.13 (9.55)	8.1 ± 0.2	4.6 ± 0.4	0.30 ± 0.09 (2.00)
I286A	7.2 ± 0.2	6.5 ± 0.8	0.65 ± 0.11 (4.47)	7.8 ± 0.2	5.7 ± 0.4	0.37 ± 0.09 (2.34)
V287A	6.9 ± 0.2	6.8 ± 0.7	0.61 ± 0.14 (4.07)	7.6 ± 0.3	5.3 ± 0.6	0.33 ± 0.13 (2.14)
K288A	6.6 ± 0.6	3.3 ± 1.1	-0.01 ± 0.38 (0.98)	**6.7 ± 0.3***	**2.9 ± 0.5***	-0.09 ± 0.28 (0.81)
Y289A	7.3 ± 0.4	4.9 ± 0.8	0.55 ± 0.11 (3.55)	7.4 ± 0.3	5.0 ± 0.6	0.31 ± 0.09 (2.04)
L290A	7.0 ± 0.2	5.5 ± 0.6	0.40 ± 0.11 (2.51)	7.9 ± 0.3	**3.4 ± 0.4***	-0.03 ± 0.10 (0.93)
Y291A	6.9 ± 0.3	5.7 ± 1.0	0.32 ± 0.12 (2.09)	7.8 ± 0.3	4.1 ± 0.4	0.02 ± 0.11 (1.05)
E292A	6.7 ± 0.3	3.9 ± 0.7	0.08 ± 0.20 (1.20)	7.2 ± 0.2	**2.0 ± 0.2***	**-0.37 ± 0.19 (0.43)***
D293A	7.2 ± 0.3	4.0 ± 0.5	0.10 ± 0.14 (1.26)	7.5 ± 0.3	**2.7 ± 0.3***	-0.18 ± 0.14 (0.66)
E294A	7.1 ± 0.2	6.0 ± 0.5	0.28 ± 0.19 (1.91)	7.8 ± 0.2	4.0 ± 0.3	-0.18 ± 0.18 (0.66)
G295A	6.9 ± 0.2	8.1 ± 0.9	0.79 ± 0.11 (6.17)	7.8 ± 0.2	5.9 ± 0.5	0.45 ± 0.09 (2.82)
C296A	7.8 ± 0.4	**2.0 ± 0.4***	-0.23 ± 0.21 (0.59)	6.9 ± 0.3	4.7 ± 0.7	0.47 ± 0.14 (2.95)
W297A	7.9 ± 0.5	**2.2 ± 0.4***	-0.21 ± 0.16 (0.62)	7.3 ± 0.4	**3.0 ± 0.5***	0.05 ± 0.14 (1.12)
T298A	7.8 ± 0.2	6.9 ± 0.5	0.91 ± 0.16 (8.13)	8.0 ± 0.2	6.1 ± 0.5	0.27 ± 0.13 (1.86)
R299A	7.5 ± 0.3	5.4 ± 0.8	0.55 ± 0.13 (3.55)	7.5 ± 0.2	4.2 ± 0.4	0.32 ± 0.10 (2.09)
N300A	**N.D.**	**N.D.**	**N.D.**	7.6 ± 0.3	**3.1 ± 0.4***	-0.30 ± 0.14 (0.50)
S301A	7.3 ± 0.2	4.8 ± 0.5	0.38 ± 0.10 (2.40)	7.8 ± 0.2	4.5 ± 0.4	0.18 ± 0.08 (1.51)
N302A	7.0 ± 0.3	5.4 ± 1.0	-0.02 ± 0.21 (0.95)	7.5 ± 0.3	4.5 ± 0.5	-0.03 ± 0.19 (0.93)
M303A	7.2 ± 0.3	5.5 ± 0.8	0.29 ± 0.16 (1.95)	7.8 ± 0.2	5.5 ± 0.4	0.32 ± 0.10 (2.09)
N304A	7.5 ± 0.2	5.8 ± 0.5	0.88 ± 0.15 (7.59)	7.9 ± 0.3	**3.2 ± 0.4***	0.12 ± 0.13 (1.32)
Y305A	7.5 ± 0.2	3.4 ± 0.3	-0.19 ± 0.14 (0.65)	7.5 ± 0.3	**3.3 ± 0.3***	-0.20 ± 0.12 (0.63)
W306A	**N.D.**	**N.D.**	**N.D.**	**N.D.**	**N.D.**	**N.D.**
L307A	7.4 ± 0.2	**2.8 ± 0.2***	-0.16 ± 0.15 (0.69)	7.6 ± 0.2	**3.1 ± 0.3***	-0.07 ± 0.10 (0.85)

* Data were statistically significant at $p < 0.05$, one-way analysis of variance, and Dunnett's post test in comparison with wild type response.

In this study we have used alanine scanning of ECL2 and adjacent residues to probe the function of this domain of the human GLP-1R. Virtually all mutations impacted on receptor function, in particular on ligand efficacy, although the nature and extent of effect varied considerably depending on the pathway, the ligand, and the mutation. Collectively, the data are indicative of a critical role for the GLP-1R ECL2 in the activation transition of the receptor. A global role for this domain in activation transition is supported by analysis of efficacy changes to mutants across the different pathways (Fig. 7). Although there are exceptions (discussed below), there was generally a good correlation between the magnitude of efficacy change for the different pathways for individual mutants, although the direction of change in the case of pERK1/2 was not always in the same direction as the other two pathways (that were almost uniformly negative) (Fig. 7). The correlations suggest that the mutations alter the ensemble of conformations formed/sampled by the receptor in response to agonists; for a subset of mutants there is greater propensity to form conformations linked to activation of pERK1/2, but this is gained at the expense of conformations linked to either cAMP formation or $Ca^{2+}{}_i$ mobilization. The almost uniform loss of $Ca^{2+}{}_i$ efficacy with individual mutations suggests that there is a high energy barrier for formation of conformations allowing coupling to this pathway, and this is consistent with the inability of GLP-1(1–36)-NH_2 to activate this pathway.

The recent solution of the crystal structure of the agonist-bound β_2-adrenergic receptor in complex with $G\alpha_s$ (71) has provided novel insight into the structural changes in the receptor that accompany activation transition. This receptor undergoes two major rearrangements on its intracellular face as follows: an outward displacement of TM6 by ~14 Å and an α-helical extension of TM5. These changes open up the receptor for interaction with the G protein. In the activated structure,

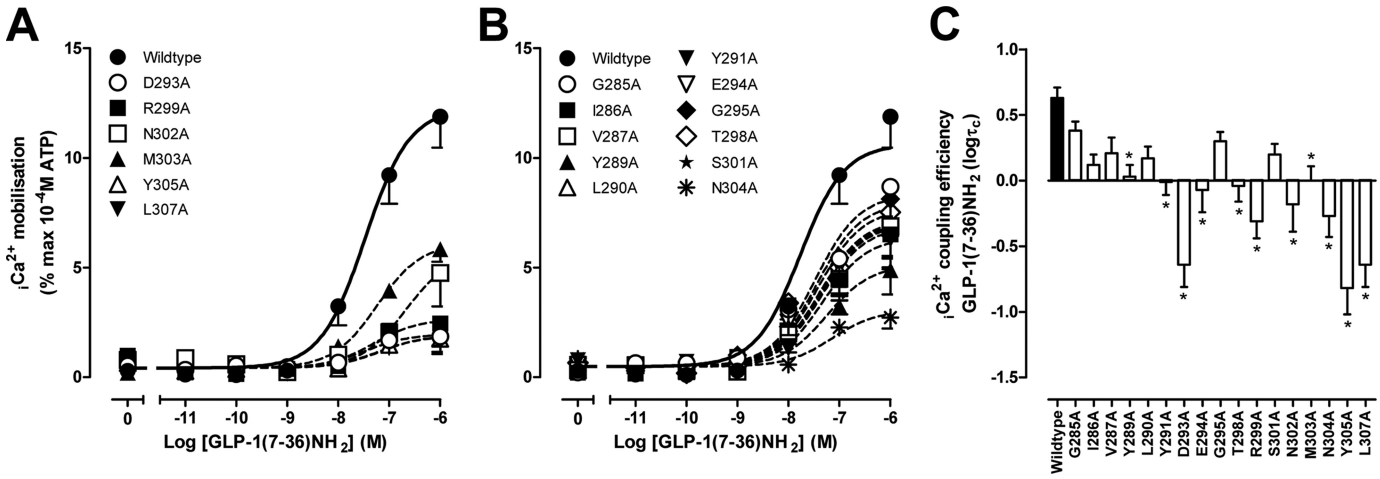

FIGURE 6. **$Ca^{2+}{}_i$ mobilization profiles of human GLP-1R ECL2 alanine mutants.** Characterization of $Ca^{2+}{}_i$ mobilization in the presence of GLP-1(7–36)-NH_2 in FlpInCHO cells stably expressing the wild type human GLP-1R or each of the human GLP-1R ECL2 alanine mutants that effect peptide binding affinity (*A*) or has no significant effect on peptide binding affinity (*B*) is shown. Data are normalized to the maximal response elicited by 100 μM ATP and analyzed with an operational model of agonism as defined in Equation 2. All values are means ± S.E. of three to five independent experiments, conducted in duplicate. Visual representation of $Ca^{2+}{}_i$ coupling efficacy ($\log\tau_c$) in the presence of GLP-1(7–36)-NH_2 (*C*) is shown. Statistical significance of changes in coupling efficacy in comparison with wild type human GLP-1R was determined by one-way analysis of variance and Dunnett's post-test and is indicated with an *asterisk* (*, $p < 0.05$). All values are $\log\tau_c$ ± S.E. of three to five independent experiments, conducted in duplicate.

the α5 helix of $G\alpha_s$ forms a network of polar interactions with TM5, and therefore, the transmission of conformational change to TM5 is likely to be very important for at least $G\alpha_s$ interactions. Our data are indicative of ECL2 playing a critical role in the activation transition of the GLP-1R, potentially via effects on the conformation of TM5. Consistent with this, there was generally greater impact of mutation to residues that were distal to the conserved Cys (Cys-296) that resides near the top of TM5.

For all mutants expressed at the cell surface, binding of the antagonist peptide exendin(9–39) was unaltered, and binding affinity changes were restricted to the high affinity agonist peptide GLP-1(7–36)-NH_2 for a subset of mutants. The interpretation of binding affinity changes for agonist peptides can be difficult. Although agonists enable the transition of the receptor to facilitate G protein binding, the ternary complex of the receptor with the G protein (or indeed with other regulatory proteins) provides thermodynamically reciprocal (allosteric) regulation of agonist binding (72). This has been empirically demonstrated for GPCRs using purified proteins, and for the β_2-adrenoreceptor, it has been demonstrated that the full conformational alteration to the receptor requires both agonist and G protein to be bound (73, 74). As such, major effects on receptor-G protein interactions will manifest as selective loss of high affinity agonist binding, such as those observed in this study, and distinguishing direct effects on peptide binding from indirect effects is problematic.

The most dramatic effects on receptor function were seen with those mutants that also had reduced affinity for GLP-1(7–36)-NH_2. For the mutants with greatest loss of apparent affinity, K288A, E292A, C296A, W297A, and N300A, there was a corresponding major loss of receptor function, although the loss of affinity alone was insufficient to account for the extent of functional loss. For the GLP-1(7–36)-NH_2 peptide, these mutations led to abolition of the $Ca^{2+}{}_i$ response and marked decrease in potency for cAMP formation. For most mutants, there was also a parallel loss in cAMP efficacy, and the exception to this was C296A, where efficacy was preserved (Tables 1–4). For GLP-1(1–36)-NH_2 there was total loss of response in cAMP formation. The effect on pERK1/2 was more complex. Lys-288, Cys-296, and Trp-297 are each very highly conserved across the B subfamily of peptide hormone GPCRs and this may indicate a structural role for these residues (Fig. 1*A*). This is supported by the loss of functional cell surface receptors seen with alanine mutants of these residues (Table 1 and Fig. 2). For Cys-296, a structural role is clearly evident with this amino acid forming a disulfide bond with Cys-226 at the top of TM3; this structural motif is highly conserved across the superfamily of GPCRs and is evident in solved crystal structures for family A GPCRs (57–61, 75, 76). In the rat GLP-1R, double mutation of Cys-226 and Cys-296 to alanine restored the loss of GLP-1(7–36)-NH_2 binding affinity and cAMP signaling seen with individual mutation of these residues, indicating that the disulfide link itself is not required for efficient activation of the receptor (77).

Recent photoaffinity cross-linking work has demonstrated that Leu-20 of GLP-1(7–36)-NH_2 is proximal to Trp-297 of the receptor, with subsequent molecular modeling indicating that it could form a direct interaction that may contribute to the loss of function observed with mutation of this residue (36). Interestingly, Leu-20 is distal to the segment of the GLP-1 peptide (and indeed other related peptide hormones) that is linked to agonistic activity. Dipeptidyl peptidase IV cleavage of the two N-terminal residues markedly attenuates the activity of GLP-1(7–36)-NH_2, and truncation by six amino acids is sufficient to abolish agonist activity (78). In this study binding affinity of the antagonist peptide exendin(9–39) was unaltered by any of the mutations, and thus it seems unlikely that the extent of loss of function seen with the W297A is due to loss of a direct interaction. It has been speculated that low binding affinity for GLP-1(7–36)-NH_2 for the isolated N-terminal extracellular domain of the GLP-1R is due to decreased capacity of GLP-1(7–36)-

TABLE 4

Effects of human GLP-1R ECL2 alanine mutants on peptide agonist signaling via $Ca^{2+}{}_i$ mobilization

Data were analyzed using a three-parameter logistic equation as defined in Equation 1. pEC_{50} values represent the negative logarithm of the concentration of agonist that produces half the maximal response. E_{max} represents the maximal response normalized to that elicited by 100 μM ATP. All mutants were analyzed with an operational model of agonism (Equation 2) to determine logτ values. All logτ values were then corrected to specific ^{125}I-exendin(9–39) binding (logτ_c). Values are expressed as means ± S.E. of three to five independent experiments, conducted in duplicate. Data were analyzed with one-way analysis of variance and Dunnett's post test The R^2 value for the global curve fit was 0.79. Gray shading highlights residues effecting peptide agonist binding affinity. ND means data were unable to be experimentally defined.

	iCa^{2+} mobilization		
	GLP-1(7-36)NH_2		
	pEC_{50}	E_{max}	logτ_c (τ_c)
Wildtype	7.5 ± 0.1	12.2 ± 0.8	0.63 ± 0.08 (4.27)
G285A	7.3 ± 0.2	**8.7 ± 0.9***	0.38 ± 0.07 (2.40)
I286A	8.0 ± 0.3	**5.9 ± 0.6***	0.12 ± 0.08 (1.32)
V287A	7.3 ± 0.2	**7.0 ± 0.7***	0.21 ± 0.12 (1.62)
K288A	**N.D.**	**N.D.**	N.D.
Y289A	7.4 ± 0.3	**4.8 ± 0.6***	**0.03 ± 0.09 (1.07)***
L290A	7.5 ± 0.2	**6.8 ± 0.7***	0.17 ± 0.09 (1.48)
Y291A	7.2 ± 0.2	**6.7 ± 0.7***	**-0.01 ± 0.10 (0.98)***
E292A	**N.D.**	**N.D.**	**N.D.**
D293A	7.5 ± 0.4	**2.0 ± 0.3***	**-0.64 ± 0.17 (0.23)***
E294A	7.6 ± 0.3	**6.6 ± 0.8***	**-0.07 ± 0.17 (0.85)***
G295A	7.3 ± 0.2	**8.3 ± 0.7***	0.30 ± 0.07 (2.00)
C296A	**N.D.**	**N.D.**	**N.D.**
W297A	**N.D.**	**N.D.**	**N.D.**
T298A	7.8 ± 0.1	**7.0 ± 0.4***	**-0.04 ± 0.12 (0.91)***
R299A	7.3 ± 0.5	**2.7 ± 0.6***	**-0.31 ± 0.13 (0.49)***
N300A	**N.D.**	**N.D.**	**N.D.**
S301A	7.6 ± 0.2	**6.7 ± 0.5***	0.20 ± 0.08 (1.58)
N302A	6.6 ± 0.4	**5.9 ± 1.4***	**-0.18 ± 0.21 (0.66)***
M303A	7.2 ± 0.1	**6.1 ± 0.4***	**0.00 ± 0.11 (1.00)***
N304A	7.3 ± 0.3	**2.9 ± 0.4***	**-0.27 ± 0.16 (0.54)***
Y305A	7.2 ± 0.4	**1.7 ± 0.3***	**-0.82 ± 0.20 (0.15)***
W306A	**N.D.**	**N.D.**	**N.D.**
L307A	7.0 ± 0.4	**2.4 ± 0.5***	**-0.64 ± 0.17 (0.23)***

* Data were statistically significant at $p < 0.05$, one-way analysis of variance, and Dunnett's post test in comparison with wild type response.

TABLE 5

Effects of human GLP-1R ECL2 alanine mutants on peptide agonist-mediated signaling bias

Data were analyzed using an operational model of agonism as defined in Equation 4 to estimate logτ_c/K_A ratios. Changes in logτ_c/K_A ratios with respect to wild type were used to quantitate bias between signaling pathways. Values are expressed as means ± S.E. of three to seven independent experiments, conducted in duplicate. Data were analyzed with one-way analysis of variance and Dunnett's post test. Gray shading highlights residues effecting peptide agonist binding affinity. ND means were data unable to be experimentally defined.

	Bias Factors			
	GLP-1(1-36)NH_2	GLP-1(7-36)NH_2		
	cAMP-ERK	cAMP-ERK	cAMP-$_i$Ca^{2+}	ERK-$_i$Ca^{2+}
Wildtype	0.00 ± 0.22	0.00 ± 0.19	0.00 ± 0.17	0.00 ± 0.21
G285A	-0.39 ± 0.23	0.02 ± 0.19	0.42 ± 0.23	0.40 ± 0.22
I286A	-0.34 ± 0.27	-0.19 ± 0.22	0.41 ± 0.19	0.59 ± 0.22
V287A	-0.44 ± 0.24	-0.29 ± 0.24	0.15 ± 0.25	0.44 ± 0.29
K288A	**N.D.**	**N.D.**	**N.D.**	**N.D.**
Y289A	0.03 ± 0.25	-0.33 ± 0.21	0.19 ± 0.36	0.52 ± 0.34
L290A	-0.45 ± 0.32	-0.43 ± 0.35	-0.07 ± 0.29	0.35 ± 0.40
Y291A	-0.38 ± 0.30	-0.60 ± 0.30	0.06 ± 0.29	0.65 ± 0.33
E292A	**N.D.**	**-1.38 ± 0.41***	**N.D.**	**N.D.**
D293A	-1.17 ± 0.35	-0.90 ± 0.33	-0.45 ± 0.60	0.45 ± 0.68
E294A	-0.22 ± 0.26	-0.03 ± 0.30	0.22 ± 0.27	0.25 ± 0.34
G295A	-0.50 ± 0.23	-0.55 ± 0.25	0.05 ± 0.20	0.60 ± 0.25
C296A	**N.D.**	**-1.51 ± 0.19***	**N.D.**	**N.D.**
W297A	**N.D.**	**-2.52 ± 0.38***	**N.D.**	**N.D.**
T298A	-0.79 ± 0.23	-0.54 ± 0.22	0.25 ± 0.18	0.80 ± 0.20
R299A	**-1.53 ± 0.43***	**-1.36 ± 0.21***	-0.72 ± 0.43	0.64 ± 0.46
N300A	**N.D.**	**-2.64 ± 0.29***	**N.D.**	**N.D.**
S301A	-0.36 ± 0.22	-0.52 ± 0.27	-0.21 ± 0.23	0.31 ± 0.30
N302A	-1.17 ± 0.33	**-1.13 ± 0.24***	-0.11 ± 0.22	1.02 ± 0.30
M303A	-0.45 ± 0.25	-0.77 ± 0.27	0.05 ± 0.24	0.82 ± 0.30
N304A	-1.07 ± 0.23	-0.69 ± 0.33	-0.02 ± 0.55	0.67 ± 0.48
Y305A	**-1.76 ± 0.46***	**-1.32 ± 0.19***	-0.47 ± 0.63	0.85 ± 0.64
W306A	**N.D.**	**N.D.**	**N.D.**	**N.D.**
L307A	-1.15 ± 0.47	**-1.25 ± 0.31***	-0.32 ± 0.56	0.93 ± 0.61

* Data were statistically significant at $p < 0.05$, one-way analysis of variance, and Dunnett's post test in comparison with wild type response.

NH_2 to form an extended α-helix in the absence of the receptor core (79). It is possible that one role of Trp-297 is to help stabilize peptide secondary structure. Nonetheless, Trp-297 is completely conserved across all B family members suggesting that it is structurally important.

Mutation of Lys-288 to alanine in the rat GLP-1R leads to a similar decrease in GLP-1(7–36)-NH_2 affinity to that observed in this study, and although a cAMP response via the rat GLP-1R is detectable, there is a marked decrease in potency. At the equivalent position in other family B receptors, this amino acid is highly conserved with an invariant basic residue (Arg or Lys) present (Fig. 1*A*). Al-Sabah and Donnelly (37) have speculated that Lys-288 likely resides at the border between TM4 and ECL2 and that a basic residue in this position is potentially required for important interactions with neighboring TM residues. Nonetheless, such basic amino acids may also reside at the hydrophobic face of TM helices and undergo what is termed "snorkeling," where the side chain is oriented parallel to the membrane helix leading to stabilization of the top of the TM helix (80), and this may be important in receptor function.

Glu-292 and Asn-300 are partially conserved across B family receptors, being homologous with more closely related members of the family (Fig. 1*A*). These receptors also have the greatest degree of homology with the N-terminal sequences of their activating peptides (Fig. 1*B*), and this may suggest more direct importance for interaction between the receptors and peptides. Although among the most deleterious of mutations for all pathways, their effect on relative efficacy across pathways is consistent with most other ECL2 mutations (Fig. 7). Nonetheless, the N300A mutant, like C296A and W297A, reversed GLP-1(7–36)-NH_2-mediated signal bias between pERK1/2 and cAMP formation (supplemental Fig. S1*B*).

Of all the mutants studied, only W306A was not expressed at the cell surface, indicating that the mutation leads to misfolding of the receptor. Curiously, double mutation of Tyr-305 and Trp-306 to alanine in the rat GLP-1R resulted in a population of receptors that were cell surface-expressed and responded to peptide agonists, albeit with marked effects on potency (77), suggesting that either interspecies differences in receptor sequence provide for greater stability of rat receptor structure or that the additional mutation compensated for some of the detrimental interactions arising from individual mutation of Trp-306.

All of the other mutations that altered the affinity of GLP-1(7–36)-NH_2, D293A, R299A, N302A, M303A, Y305A, and

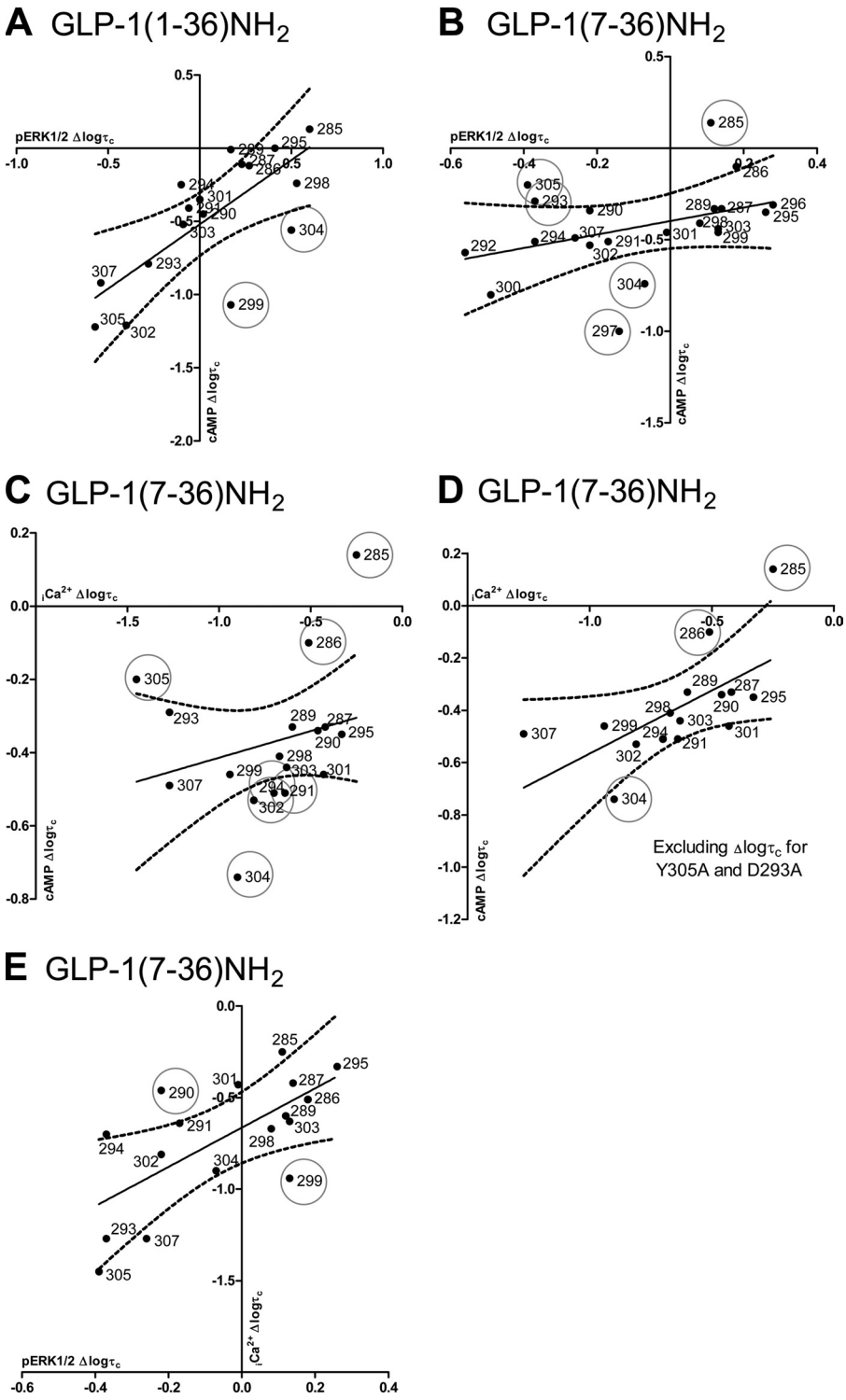

FIGURE 7. **Correlation plots of pathway efficacy (logτ_c) of human GLP-1R ECL2 alanine mutants.** Correlation plots of changes in pathway coupling efficacy (logτ_c) of human GLP-1R ECL2 alanine mutants with respect to wild type receptor are shown. *A,* cAMP *versus* pERK1/2 for GLP-1(1–36)-NH_2; *B,* cAMP *versus* pERK1/2 for GLP-1(7–36)-NH_2; *C,* $Ca^{2+}{}_i$ *versus* cAMP for GLP-1(7–36)-NH_2; *D,* $Ca^{2+}{}_i$ *versus* cAMP for GLP-1(7–36)-NH_2 after exclusion of D293A and Y305A; and *E,* pERK1/2 *versus* $Ca^{2+}{}_i$ for GLP-1(7–36)-NH_2. Data were fit by linear regression. The line of regression and 99% confidence intervals are displayed.

L307A were among those residues that conferred the largest differential effects on either signal bias (supplemental Fig. S1) or magnitude of change to efficacy across pathways (Fig. 7). Of the other mutants within ECL2, which did not alter GLP-1(7–36)-NH_2 affinity, only N304A that is near the apex of TM5 caused significant differential effects across signaling pathways. These data are indicative of a novel and important role for ECL2 in conferring the distinct conformations that underlie pathway selective signaling. Whether this occurs purely through effects on the conformation of TM5 or whether additional interactions of ECL2 residues with other loop regions are involved is unclear.

The two GLP-1 peptides used in this study differ only by a six-amino acid extension to the GLP-1(7–36)-NH_2 sequence. Not surprisingly, most mutations had similar effects on responses to both peptides. Nonetheless, GLP-1(1–36)-NH_2 exhibits distinct signal bias to that demonstrated by GLP-1(7–36)-NH_2, indicating that it produces a different ensemble of receptor conformations to that of the truncated peptide. Consistent with the effects of the different peptides in altering receptor bias, C296A, R299A, N302A, N304A, and Y305A had differential effects on the truncated and full-length GLP-1 peptides. Differential effects were also seen with the G285A mutant. Both peptides displayed increased efficacy at this mutant receptor; however, greater improvement in pERK1/2 efficacy was seen for GLP-1(1–36)-NH_2 relative to GLP-1(7–36)-NH_2. Alanine at this position may thus provide some conformational restriction that allows the lower affinity full-length peptide to more readily activate the pERK1/2 pathway compared with the wild type receptor.

In conclusion, we have demonstrated a critical role for ECL2 in activation of the GLP-1R. However, the precise molecular mechanisms driving these effects remain elusive in the absence of high resolution structural information for family B GPCRs. Our data point to a major role for ECL2 in activation transition and that changes to structure in this receptor region can alter pathway bias of the receptor that can be manifested in a ligand-specific manner.

REFERENCES

1. Harmar, A. J., Hills, R. A., Rosser, E. M., Jones, M., Buneman, O. P., Dunbar, D. R., Greenhill, S. D., Hale, V. A., Sharman, J. L., Bonner, T. I., Catterall, W. A., Davenport, A. P., Delagrange, P., Dollery, C. T., Foord, S. M., Gutman, G. A., Laudet, V., Neubig, R. R., Ohlstein, E. H., Olsen, R. W., Peters, J., Pin, J. P., Ruffolo, R. R., Searls, D. B., Wright, M. W., and Spedding, M. (2009) IUPHAR-DB. The IUPHAR database of G protein-coupled receptors and ion channels. *Nucleic Acids Res.* **37,** D680–D685
2. Overington, J. P., Al-Lazikani, B., and Hopkins, A. L. (2006) How many drug targets are there? *Nat. Rev. Drug Discov.* **5,** 993–996
3. Bazarsuren, A., Grauschopf, U., Wozny, M., Reusch, D., Hoffmann, E., Schaefer, W., Panzner, S., and Rudolph, R. (2002) *In vitro* folding, functional characterization, and disulfide pattern of the extracellular domain of human GLP-1 receptor. *Biophys. Chem.* **96,** 305–318
4. Grauschopf, U., Lilie, H., Honold, K., Wozny, M., Reusch, D., Esswein, A., Schäfer, W., Rücknagel, K. P., and Rudolph, R. (2000) The N-terminal fragment of human parathyroid hormone receptor 1 constitutes a hormone binding domain and reveals a distinct disulfide pattern. *Biochemistry* **39,** 8878–8887
5. Bisello, A., Adams, A. E., Mierke, D. F., Pellegrini, M., Rosenblatt, M., Suva, L. J., and Chorev, M. (1998) Parathyroid hormone-receptor interactions identified directly by photocross-linking and molecular modeling studies. *J. Biol. Chem.* **273,** 22498–22505
6. Dong, M., Li, Z., Pinon, D. I., Lybrand, T. P., and Miller, L. J. (2004) Spatial approximation between the amino terminus of a peptide agonist and the top of the sixth transmembrane segment of the secretin receptor. *J. Biol. Chem.* **279,** 2894–2903
7. Dong, M., Pinon, D. I., Cox, R. F., and Miller, L. J. (2004) Molecular approximation between a residue in the amino-terminal region of calcitonin and the third extracellular loop of the class B G protein-coupled calcitonin receptor. *J. Biol. Chem.* **279,** 31177–31182
8. Hoare, S. R. (2005) Mechanisms of peptide and nonpeptide ligand binding to Class B G-protein-coupled receptors. *Drug Discov. Today* **10,** 417–427
9. Bergwitz, C., Gardella, T. J., Flannery, M. R., Potts, J. T., Jr., Kronenberg, H. M., Goldring, S. R., and Jüppner, H. (1996) Full activation of chimeric receptors by hybrids between parathyroid hormone and calcitonin. Evidence for a common pattern of ligand-receptor interaction. *J. Biol. Chem.* **271,** 26469–26472
10. Graziano, M. P., Hey, P. J., and Strader, C. D. (1996) The amino-terminal domain of the glucagon-like peptide-1 receptor is a critical determinant of subtype specificity. *Receptors Channels* **4,** 9–17
11. Holtmann, M. H., Hadac, E. M., and Miller, L. J. (1995) Critical contributions of amino-terminal extracellular domains in agonist binding and activation of secretin and vasoactive intestinal polypeptide receptors. Studies of chimeric receptors. *J. Biol. Chem.* **270,** 14394–14398
12. Wilmen, A., Göke, B., and Göke, R. (1996) The isolated N-terminal extracellular domain of the glucagon-like peptide-1 (GLP)-1 receptor has intrinsic binding activity. *FEBS Lett.* **398,** 43–47
13. Wilmen, A., Van Eyll, B., Göke, B., and Göke, R. (1997) Five out of six tryptophan residues in the N-terminal extracellular domain of the rat GLP-1 receptor are essential for its ability to bind GLP-1. *Peptides* **18,** 301–305
14. Gelling, R. W., Wheeler, M. B., Xue, J., Gyomorey, S., Nian, C., Pederson, R. A., and McIntosh, C. H. (1997) Localization of the domains involved in ligand binding and activation of the glucose-dependent insulinotropic polypeptide receptor. *Endocrinology* **138,** 2640–2643
15. Castro, M., Nikolaev, V. O., Palm, D., Lohse, M. J., and Vilardaga, J. P. (2005) Turn-on switch in parathyroid hormone receptor by a two-step parathyroid hormone binding mechanism. *Proc. Natl. Acad. Sci. U.S.A.* **102,** 16084–16089
16. Bergwitz, C., Jusseaume, S. A., Luck, M. D., Jüppner, H., and Gardella, T. J. (1997) Residues in the membrane-spanning and extracellular loop regions of the parathyroid hormone (PTH)-2 receptor determine signaling selectivity for PTH and PTH-related peptide. *J. Biol. Chem.* **272,** 28861–28868
17. Hjorth, S. A., Adelhorst, K., Pedersen, B. B., Kirk, O., and Schwartz, T. W. (1994) Glucagon and glucagon-like peptide 1. Selective receptor recognition via distinct peptide epitopes. *J. Biol. Chem.* **269,** 30121–30124
18. Holtmann, M. H., Ganguli, S., Hadac, E. M., Dolu, V., and Miller, L. J. (1996) Multiple extracellular loop domains contribute critical determinants for agonist binding and activation of the secretin receptor. *J. Biol. Chem.* **271,** 14944–14949
19. Buggy, J. J., Livingston, J. N., Rabin, D. U., and Yoo-Warren, H. (1995) Glucagon·glucagon-like peptide I receptor chimeras reveal domains that determine specificity of glucagon binding. *J. Biol. Chem.* **270,** 7474–7478
20. Xiao, Q., Jeng, W., and Wheeler, M. B. (2000) Characterization of glucagon-like peptide-1 receptor-binding determinants. *J. Mol. Endocrinol.* **25,** 321–335
21. Adelhorst, K., Hedegaard, B. B., Knudsen, L. B., and Kirk, O. (1994) Structure-activity studies of glucagon-like peptide-1. *J. Biol. Chem.* **269,** 6275–6278
22. Mojsov, S. (1992) Structural requirements for biological activity of glucagon-like peptide-I. *Int. J. Pept. Protein Res.* **40,** 333–343
23. Nicole, P., Lins, L., Rouyer-Fessard, C., Drouot, C., Fulcrand, P., Thomas, A., Couvineau, A., Martinez, J., Brasseur, R., and Laburthe, M. (2000) Identification of key residues for interaction of vasoactive intestinal peptide with human VPAC1 and VPAC2 receptors and development of a highly selective VPAC1 receptor agonist. Alanine scanning and molecular modeling of the peptide. *J. Biol. Chem.* **275,** 24003–24012
24. Dong, M., Le, A., Te, J. A., Pinon, D. I., Bordner, A. J., and Miller, L. J. (2011) Importance of each residue within secretin for receptor binding and biological activity. *Biochemistry* **50,** 2983–2993
25. Runge, S., Wulff, B. S., Madsen, K., Bräuner-Osborne, H., and Knudsen, L. B. (2003) Different domains of the glucagon and glucagon-like peptide-1 receptors provide the critical determinants of ligand selectivity. *Br. J. Pharmacol.* **138,** 787–794
26. Runge, S., Gram, C., Brauner-Osborne, H., Madsen, K., Knudsen, L. B., and Wulff, B. S. (2003) Three distinct epitopes on the extracellular face of the glucagon receptor determine specificity for the glucagon amino terminus. *J. Biol. Chem.* **278,** 28005–28010
27. Parthier, C., Kleinschmidt, M., Neumann, P., Rudolph, R., Manhart, S., Schlenzig, D., Fanghänel, J., Rahfeld, J. U., Demuth, H. U., and Stubbs, M. T. (2007) Crystal structure of the incretin-bound extracellular domain of a G protein-coupled receptor. *Proc. Natl. Acad. Sci. U.S.A.* **104,** 13942–13947

28. Grace, C. R., Perrin, M. H., DiGruccio, M. R., Miller, C. L., Rivier, J. E., Vale, W. W., and Riek, R. (2004) NMR structure and peptide hormone-binding site of the first extracellular domain of a type B1 G protein-coupled receptor. *Proc. Natl. Acad. Sci. U.S.A.* **101,** 12836–12841
29. Grace, C. R., Perrin, M. H., Gulyas, J., Digruccio, M. R., Cantle, J. P., Rivier, J. E., Vale, W. W., and Riek, R. (2007) Structure of the N-terminal domain of a type B1 G protein-coupled receptor in complex with a peptide ligand. *Proc. Natl. Acad. Sci. U.S.A.* **104,** 4858–4863
30. Pioszak, A. A., Parker, N. R., Suino-Powell, K., and Xu, H. E. (2008) Molecular recognition of corticotropin-releasing factor by its G-protein-coupled receptor CRFR1. *J. Biol. Chem.* **283,** 32900–32912
31. Pioszak, A. A., and Xu, H. E. (2008) Molecular recognition of parathyroid hormone by its G protein-coupled receptor. *Proc. Natl. Acad. Sci. U.S.A.* **105,** 5034–5039
32. Runge, S., Thøgersen, H., Madsen, K., Lau, J., and Rudolph, R. (2008) Crystal structure of the ligand-bound glucagon-like peptide-1 receptor extracellular domain. *J. Biol. Chem.* **283,** 11340–11347
33. Underwood, C. R., Garibay, P., Knudsen, L. B., Hastrup, S., Peters, G. H., Rudolph, R., and Reedtz-Runge, S. (2010) Crystal structure of glucagon-like peptide-1 in complex with the extracellular domain of the glucagon-like peptide-1 receptor. *J. Biol. Chem.* **285,** 723–730
34. López de Maturana, R., and Donnelly, D. (2002) The glucagon-like peptide-1 receptor binding site for the N-terminus of GLP-1 requires polarity at Asp-198 rather than negative charge. *FEBS Lett.* **530,** 244–248
35. López de Maturana, R., Treece-Birch, J., Abidi, F., Findlay, J. B., and Donnelly, D. (2004) Met-204 and Tyr-205 are together important for binding GLP-1 receptor agonists but not their N-terminally truncated analogues. *Protein Pept. Lett.* **11,** 15–22
36. Miller, L. J., Chen, Q., Lam, P. C., Pinon, D. I., Sexton, P. M., Abagyan, R., and Dong, M. (2011) Refinement of glucagon-like peptide 1 docking to its intact receptor using mid-region photolabile probes and molecular modeling. *J. Biol. Chem.* **286,** 15895–15907
37. Al-Sabah, S., and Donnelly, D. (2003) The positive charge at Lys-288 of the glucagon-like peptide-1 (GLP-1) receptor is important for binding the N-terminus of peptide agonists. *FEBS Lett.* **553,** 342–346
38. Assil-Kishawi, I., and Abou-Samra, A. B. (2002) Sauvagine cross-links to the second extracellular loop of the corticotropin-releasing factor type 1 receptor. *J. Biol. Chem.* **277,** 32558–32561
39. Liaw, C. W., Grigoriadis, D. E., Lovenberg, T. W., De Souza, E. B., and Maki, R. A. (1997) Localization of ligand-binding domains of human corticotropin-releasing factor receptor. A chimeric receptor approach. *Mol. Endocrinol.* **11,** 980–985
40. Baggio, L. L., and Drucker, D. J. (2007) Biology of incretins. GLP-1 and GIP. *Gastroenterology* **132,** 2131–2157
41. Quoyer, J., Longuet, C., Broca, C., Linck, N., Costes, S., Varin, E., Bockaert, J., Bertrand, G., and Dalle, S. (2010) GLP-1 mediates antiapoptotic effect by phosphorylating Bad through a β-arrestin 1-mediated ERK1/2 activation in pancreatic beta-cells. *J. Biol. Chem.* **285,** 1989–2002
42. Klinger, S., Poussin, C., Debril, M. B., Dolci, W., Halban, P. A., and Thorens, B. (2008) Increasing GLP-1-induced beta-cell proliferation by silencing the negative regulators of signaling cAMP-response element modulator-α and DUSP14. *Diabetes* **57,** 584–593
43. Drucker, D. J., and Nauck, M. A. (2006) The incretin system. Glucagon-like peptide-1 receptor agonists and dipeptidyl peptidase-4 inhibitors in type 2 diabetes. *Lancet* **368,** 1696–1705
44. May, L. T., Avlani, V. A., Langmead, C. J., Herdon, H. J., Wood, M. D., Sexton, P. M., and Christopoulos, A. (2007) Structure-function studies of allosteric agonism at M2 muscarinic acetylcholine receptors. *Mol. Pharmacol.* **72,** 463–476
45. Koole, C., Wootten, D., Simms, J., Valant, C., Miller, L. J., Christopoulos, A., and Sexton, P. M. (2011) Polymorphism and ligand-dependent changes in human glucagon-like peptide-1 receptor (GLP-1R) function: allosteric rescue of loss of function mutation. *Mol. Pharmacol.* **80,** 486–497
46. Koole, C., Wootten, D., Simms, J., Valant, C., Sridhar, R., Woodman, O. L., Miller, L. J., Summers, R. J., Christopoulos, A., and Sexton, P. M. (2010) Allosteric ligands of the glucagon-like peptide 1 receptor (GLP-1R) differentially modulate endogenous and exogenous peptide responses in a pathway-selective manner: implications for drug screening. *Mol. Pharmacol.* **78,** 456–465
47. Werry, T. D., Gregory, K. J., Sexton, P. M., and Christopoulos, A. (2005) Characterization of serotonin 5-HT2C receptor signaling to extracellular signal-regulated kinases 1 and 2. *J. Neurochem.* **93,** 1603–1615
48. Cheng, Y., and Prusoff, W. H. (1973) Relationship between the inhibition constant (K_1) and the concentration of inhibitor which causes 50% inhibition (I_{50}) of an enzymatic reaction. *Biochem. Pharmacol.* **22,** 3099–3108
49. Black, J. W., and Leff, P. (1983) Operational models of pharmacological agonism. *Proc. R. Soc. Lond. B Biol. Sci.* **220,** 141–162
50. Gregory, K. J., Hall, N. E., Tobin, A. B., Sexton, P. M., and Christopoulos, A. (2010) Identification of orthosteric and allosteric site mutations in M2 muscarinic acetylcholine receptors that contribute to ligand-selective signaling bias. *J. Biol. Chem.* **285,** 7459–7474
51. Figueroa, K. W., Griffin, M. T., and Ehlert, F. J. (2009) Selectivity of agonists for the active state of M1 to M4 muscarinic receptor subtypes. *J. Pharmacol. Exp. Ther.* **328,** 331–342
52. Luttrell, L. M., Ferguson, S. S., Daaka, Y., Miller, W. E., Maudsley, S., Della Rocca, G. J., Lin, F., Kawakatsu, H., Owada, K., Luttrell, D. K., Caron, M. G., and Lefkowitz, R. J. (1999) β-Arrestin-dependent formation of β2-adrenergic receptor-Src protein kinase complexes. *Science* **283,** 655–661
53. DeFea, K. A., Zalevsky, J., Thoma, M. S., Déry, O., Mullins, R. D., and Bunnett, N. W. (2000) β-Arrestin-dependent endocytosis of proteinase-activated receptor 2 is required for intracellular targeting of activated ERK1/2. *J. Cell Biol.* **148,** 1267–1281
54. Luttrell, L. M., Roudabush, F. L., Choy, E. W., Miller, W. E., Field, M. E., Pierce, K. L., and Lefkowitz, R. J. (2001) Activation and targeting of extracellular signal-regulated kinases by β-arrestin scaffolds. *Proc. Natl. Acad. Sci. U.S.A.* **98,** 2449–2454
55. Shenoy, S. K., Drake, M. T., Nelson, C. D., Houtz, D. A., Xiao, K., Madabushi, S., Reiter, E., Premont, R. T., Lichtarge, O., and Lefkowitz, R. J. (2006) β-Arrestin-dependent, G protein-independent ERK1/2 activation by the β2-adrenergic receptor. *J. Biol. Chem.* **281,** 1261–1273
56. Pearson, G., Robinson, F., Beers Gibson, T., Xu, B. E., Karandikar, M., Berman, K., and Cobb, M. H. (2001) Mitogen-activated protein (MAP) kinase pathways. Regulation and physiological functions. *Endocr. Rev.* **22,** 153–183
57. Warne, T., Serrano-Vega, M. J., Baker, J. G., Moukhametzianov, R., Edwards, P. C., Henderson, R., Leslie, A. G., Tate, C. G., and Schertler, G. F. (2008) Structure of a β1-adrenergic G-protein-coupled receptor. *Nature* **454,** 486–491
58. Palczewski, K., Kumasaka, T., Hori, T., Behnke, C. A., Motoshima, H., Fox, B. A., Le Trong, I., Teller, D. C., Okada, T., Stenkamp, R. E., Yamamoto, M., and Miyano, M. (2000) Crystal structure of rhodopsin. A G protein-coupled receptor. *Science* **289,** 739–745
59. Cherezov, V., Rosenbaum, D. M., Hanson, M. A., Rasmussen, S. G., Thian, F. S., Kobilka, T. S., Choi, H. J., Kuhn, P., Weis, W. I., Kobilka, B. K., and Stevens, R. C. (2007) High resolution crystal structure of an engineered human β2-adrenergic G protein-coupled receptor. *Science* **318,** 1258–1265
60. Chien, E. Y., Liu, W., Zhao, Q., Katritch, V., Han, G. W., Hanson, M. A., Shi, L., Newman, A. H., Javitch, J. A., Cherezov, V., and Stevens, R. C. (2010) Structure of the human dopamine D3 receptor in complex with a D2/D3 selective antagonist. *Science* **330,** 1091–1095
61. Jaakola, V. P., Griffith, M. T., Hanson, M. A., Cherezov, V., Chien, E. Y., Lane, J. R., Ijzerman, A. P., and Stevens, R. C. (2008) The 2.6 Å crystal structure of a human A2A adenosine receptor bound to an antagonist. *Science* **322,** 1211–1217
62. Ahn, K. H., Bertalovitz, A. C., Mierke, D. F., and Kendall, D. A. (2009) Dual role of the second extracellular loop of the cannabinoid receptor 1. Ligand binding and receptor localization. *Mol. Pharmacol.* **76,** 833–842
63. Avlani, V. A., Gregory, K. J., Morton, C. J., Parker, M. W., Sexton, P. M., and Christopoulos, A. (2007) Critical role for the second extracellular loop in the binding of both orthosteric and allosteric G protein-coupled receptor ligands. *J. Biol. Chem.* **282,** 25677–25686
64. Conner, M., Hawtin, S. R., Simms, J., Wootten, D., Lawson, Z., Conner, A. C., Parslow, R. A., and Wheatley, M. (2007) Systematic analysis of the entire second extracellular loop of the V(1a) vasopressin receptor. Key

residues, conserved throughout a G-protein-coupled receptor family, identified. *J. Biol. Chem.* **282,** 17405–17412
65. Scarselli, M., Li, B., Kim, S. K., and Wess, J. (2007) Multiple residues in the second extracellular loop are critical for M3 muscarinic acetylcholine receptor activation. *J. Biol. Chem.* **282,** 7385–7396
66. Shi, L., and Javitch, J. A. (2004) The second extracellular loop of the dopamine D2 receptor lines the binding-site crevice. *Proc. Natl. Acad. Sci. U.S.A.* **101,** 440–445
67. Ahuja, S., Hornak, V., Yan, E. C., Syrett, N., Goncalves, J. A., Hirshfeld, A., Ziliox, M., Sakmar, T. P., Sheves, M., Reeves, P. J., Smith, S. O., and Eilers, M. (2009) Helix movement is coupled to displacement of the second extracellular loop in rhodopsin activation. *Nat. Struct. Mol. Biol.* **16,** 168–175
68. abu Alla, S., Quitterer, U., Grigoriev, S., Maidhof, A., Haasemann, M., Jarnagin, K., and Müller-Esterl, W. (1996) Extracellular domains of the bradykinin B2 receptor involved in ligand binding and agonist sensing defined by anti-peptide antibodies. *J. Biol. Chem.* **271,** 1748–1755
69. Lebesgue, D., Wallukat, G., Mijares, A., Granier, C., Argibay, J., and Hoebeke, J. (1998) An agonist-like monoclonal antibody against the human β2-adrenoceptor. *Eur. J. Pharmacol.* **348,** 123–133
70. Ott, T. R., Troskie, B. E., Roeske, R. W., Illing, N., Flanagan, C. A., and Millar, R. P. (2002) Two mutations in extracellular loop 2 of the human GnRH receptor convert an antagonist to an agonist. *Mol. Endocrinol.* **16,** 1079–1088
71. Rasmussen, S. G., Devree, B. T., Zou, Y., Kruse, A. C., Chung, K. Y., Kobilka, T. S., Thian, F. S., Chae, P. S., Pardon, E., Calinski, D., Mathiesen, J. M., Shah, S. T., Lyons, J. A., Caffrey, M., Gellman, S. H., Steyaert, J., Skiniotis, G., Weis, W. I., Sunahara, R. K., and Kobilka, B. K. (2011) Crystal structure of the β2 adrenergic receptor-Gs protein complex. *Nature* **477,** 549–555
72. Christopoulos, A., and Kenakin, T. (2002) G protein-coupled receptor allosterism and complexing. *Pharmacol. Rev.* **54,** 323–374
73. Rosenbaum, D. M., Zhang, C., Lyons, J. A., Holl, R., Aragao, D., Arlow, D. H., Rasmussen, S. G., Choi, H. J., Devree, B. T., Sunahara, R. K., Chae, P. S., Gellman, S. H., Dror, R. O., Shaw, D. E., Weis, W. I., Caffrey, M., Gmeiner, P., and Kobilka, B. K. (2011) Structure and function of an irreversible agonist-β(2) adrenoceptor complex. *Nature* **469,** 236–240
74. Rasmussen, S. G., Choi, H. J., Fung, J. J., Pardon, E., Casarosa, P., Chae, P. S., Devree, B. T., Rosenbaum, D. M., Thian, F. S., Kobilka, T. S., Schnapp, A., Konetzki, I., Sunahara, R. K., Gellman, S. H., Pautsch, A., Steyaert, J., Weis, W. I., and Kobilka, B. K. (2011) Structure of a nanobody-stabilized active state of the β(2) adrenoceptor. *Nature* **469,** 175–180
75. Shimamura, T., Shiroishi, M., Weyand, S., Tsujimoto, H., Winter, G., Katritch, V., Abagyan, R., Cherezov, V., Liu, W., Han, G. W., Kobayashi, T., Stevens, R. C., and Iwata, S. (2011) Structure of the human histamine H1 receptor complex with doxepin. *Nature* **475,** 65–70
76. Wu, B., Chien, E. Y., Mol, C. D., Fenalti, G., Liu, W., Katritch, V., Abagyan, R., Brooun, A., Wells, P., Bi, F. C., Hamel, D. J., Kuhn, P., Handel, T. M., Cherezov, V., and Stevens, R. C. (2010) Structures of the CXCR4 chemokine GPCR with small molecule and cyclic peptide antagonists. *Science* **330,** 1066–1071
77. Mann, R. J., Al-Sabah, S., de Maturana, R. L., Sinfield, J. K., and Donnelly, D. (2010) Functional coupling of Cys-226 and Cys-296 in the glucagon-like peptide-1 (GLP-1) receptor indicates a disulfide bond that is close to the activation pocket. *Peptides* **31,** 2289–2293
78. Montrose-Rafizadeh, C., Yang, H., Rodgers, B. D., Beday, A., Pritchette, L. A., and Eng, J. (1997) High potency antagonists of the pancreatic glucagon-like peptide-1 receptor. *J. Biol. Chem.* **272,** 21201–21206
79. Mann, R. J., Nasr, N. E., Sinfield, J. K., Paci, E., and Donnelly, D. (2010) The major determinant of exendin-4/glucagon-like peptide 1 differential affinity at the rat glucagon-like peptide 1 receptor N-terminal domain is a hydrogen bond from SER-32 of exendin-4. *Br. J. Pharmacol.* **160,** 1973–1984
80. Segrest, J. P., De Loof, H., Dohlman, J. G., Brouillette, C. G., and Anantharamaiah, G. M. (1990) Amphipathic helix motif. Classes and properties. *Proteins* **8,** 103–117

Second Extracellular Loop of Human Glucagon-like Peptide-1 Receptor (GLP-1R) Has a Critical Role in GLP-1 Peptide Binding and Receptor Activation

Cassandra Koole, Denise Wootten, John Simms, Laurence J. Miller, Arthur Christopoulos and Patrick M. Sexton

J. Biol. Chem. 2012, 287:3642-3658.
doi: 10.1074/jbc.M111.309328 originally published online December 6, 2011